OPEN ACCESS

Scholars International Journal of Chemistry and Material Sciences

Abbreviated Key Title: Sch Int J Chem Mater Sci
ISSN 2616-8669 (Print) |ISSN 2617-6556 (Online)
Scholars Middle East Publishers, Dubai, United Arab Emirates
Journal homepage: http://saudijournals.com

Review Article

Deuterated Detergents for Structure-Function Analysis of Membrane Proteins in Solution Using Nuclear Magnetic Resonance (NMR) Spectroscopy and Small-Angle Neutron Scattering (SANS)

Kazumi Hiruma-Shimizu[1], Hiroki Shimizu[2], Nighat Nawaz[3], Gary S. Thompson[4], Jennifer H. Tomlinson[5], Arnout P. Kalverda[6], Simon G. Patching[7]*

[1]Waseda University, Tokyo 169-8050, Japan
[2]National Institute of Advanced Industrial Science and Technology, Hokkaido 062-0052, Japan
[3]Department of Chemistry, Islamia College Peshawar, Peshawar 25120, Pakistan
[4]School of Biosciences, University of Kent, Canterbury CT2 7NZ, UK
[5]School of Molecular and Cellular Biology, University of Leeds, Leeds LS2 9JT, UK
[6]Astbury Centre for Structural Molecular Biology, University of Leeds, Leeds LS2 9JT, UK
[7]School of Biomedical Sciences (Astbury Building), University of Leeds, Leeds LS2 9JT, UK

DOI: https://doi.org/10.36348/sijcms.2025.v08i04.001 | **Received:** 05.06.2025 | **Accepted:** 11.08.2025 | **Published:** 19.08.2025

***Corresponding author:** Simon G. Patching
School of Biomedical Sciences (Astbury Building), University of Leeds, Leeds LS2 9JT, UK

Abstract

Detergents are amphiphilic compounds with crucial roles in the extraction, purification and stabilization of integral membrane proteins and in experimental studies of their structure and function. One technique that is highly dependent on detergents for solubilization of membrane proteins is solution-state nuclear magnetic resonance (NMR) spectroscopy, where detergent micelles often serve as the best membrane mimetic for achieving particle sizes that tumble fast enough to produce high-resolution/high-sensitivity spectra. The best quality NMR spectra use detergents with partial or complete deuteration, which eliminate interfering proton signals from the detergent itself and eliminate potential proton relaxation pathways and strong dipole-dipole interactions that contribute line broadening effects. Another technique for which deuterated detergents have been crucial to obtain structural information about membrane proteins in solution is small-angle neutron scattering (SANS). Use of a deuterated detergent exploits the intrinsic neutron scattering length difference between hydrogen and deuterium, such that detergent is matched-out in D_2O and only signal from the membrane protein remains visible in the scattering profile, simplifying data analysis. We provide an updated review on the properties, chemical synthesis and applications of detergents that are commercially available and/or that have been synthesized with partial or complete deuteration, and that have been used in NMR or SANS studies on membrane proteins. Specifically, the detergents are sodium dodecyl sulphate (SDS), lauryldimethylamine-oxide (LDAO), *n*-octyl-β-*D*-glucoside (β-OG), *n*-dodecyl-β-*D*-maltoside (DDM) and fos-cholines including dodecylphosphocholine (DPC). We also consider effects of deuteration, detergent screening and guidelines for detergent selection.

Keywords: Detergents, Deuteration, Membrane proteins, NMR, SANS, Synthesis.

Copyright © 2025 The Author(s): This is an open-access article distributed under the terms of the Creative Commons Attribution **4.0 International License (CC BY-NC 4.0)** which permits unrestricted use, distribution, and reproduction in any medium for non-commercial use provided the original author and source are credited.

1. INTRODUCTION

Detergents are amphiphilic compounds usually having a well-defined hydrophilic domain often referred to as the 'hydrophilic head' and a separate hydrophobic domain often referred to as the 'hydrophobic tail' (Figure 1A). The high aqueous solubility of detergent molecules, as monomers and as micelles or when associated with other molecules, has given them a crucial role in the extraction, purification and stabilization of integral membrane proteins and in experimental studies of their structure and function [1-20]. The detergent molecules act as a membrane mimetic by surrounding the membrane protein in a protein-detergent micelle complex (Figure 1B) that solubilizes and/or stabilizes them in an aqueous environment and therefore allows them to be used in a wide range of experimental techniques, including X-ray crystallography, cryo-electron microscopy (cryoEM), mass spectrometry and

nuclear magnetic resonance (NMR) spectroscopy. Under such conditions, care must be taken as to what extent the native structure and functional activity of the protein is retained. There are of course a number of other membrane mimetics used in the final stages of experimental studies with membrane proteins including organic solvents, lipids, bicelles, nanodiscs, styrene maleic acid polymers (SMALPs), fluorinated surfactants and amphipols [20-39] which have different advantages and disadvantages, but this review is limited to detergent micelles. Even with these alternative membrane mimetics, detergents are often still used during the early stages of experimental procedures with membrane proteins, for example in initial solubilization from the native membrane.

One technique that has been highly dependent on detergents for structural and functional studies of integral membrane proteins is solution-state NMR spectroscopy. Detergents often provide the best solubility, stability, isotropic and homogenous samples, and particle sizes that tumble fast enough for achieving high-resolution and high-sensitivity NMR spectra. Detergent samples are also generally more straightforward to prepare than those using other membrane mimetics. Indeed, the large majority of integral membrane protein structures determined by solution-state NMR have used proteins solubilized in detergent micelles [6, 40-48]. Assessments of the prevalence of detergent types in membrane structural biology revealed that approximately 40% of 115 membrane protein structures determined by NMR were prepared in dodecylphosphocholine (DPC) micelles, whilst nearly 40% of 1200 membrane protein structures determined by X-ray crystallography were in the sugar-based detergents *n*-octyl-β-*D*-glucoside (β-OG), *n*-decyl-β-*D*-maltoside or *n*-dodecyl-β-*D*-maltoside (DDM) [49-51]. The most prolific detergents that have historically been used in experimental studies are not necessarily the best for retaining the native structure and functional activity of the protein, however. For example, it was realized that alkyl phosphocholine detergents, such as DPC, often have destabilizing and denaturing effects on integral membrane proteins, especially those with an α-helical structure [51].

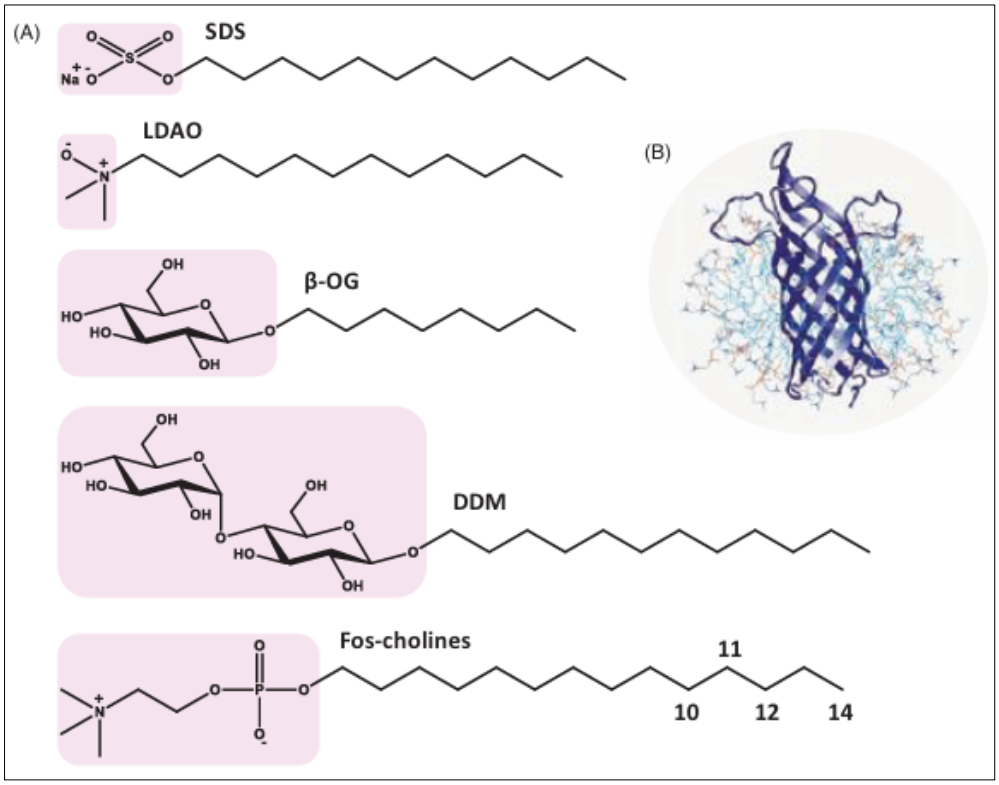

Figure 1: Structures of detergents and of a protein-micelle complex. A. Chemical structures of the detergents sodium dodecyl sulphate (SDS), lauryldimethylamine-oxide (LDAO), *n*-octyl-β-*D*-glucoside (β-OG), *n*-dodecyl-β-*D*-maltoside (DDM) and fos-cholines-10, -11, -12 and-14. The pink areas indicate the hydrophilic head groups. B. Illustration of a protein-detergent micelle complex: Molecular dynamics simulation of the outer membrane β-barrel protein OmpA from *Escherichia coli* in a dodecylphosphocholine (DPC) micelle. This Figure was reproduced from Hiruma-Shimizu *et al.,* (2015) [12].

In many solution-state NMR studies on membrane proteins, detergents with partial deuteration or complete deuteration (perdeuteration) have been used. This is because deuterated detergents eliminate interfering proton signals in NMR spectra that come from the detergent itself, which can be very intense and

not easily removed by the NMR pulse sequence. They also eliminate potential proton relaxation pathways and strong dipole-dipole interactions that would otherwise contribute to line broadening effects on the spectra. Using deuterated detergents therefore provides better resolution and sensitivity, access to overlapped areas of the protein spectrum and simplifies the application of more advanced pulse sequences [12]. The potential benefits from using deuterated detergents for NMR studies of membrane proteins were first demonstrated with the 26-residue amphiphilic peptide melittin bound to fully deuterated DPC micelles [52, 53]. These conditions allowed an almost complete assignment of ^{1}H NMR resonances and the measurement of ^{1}H-^{1}H nuclear Overhauser effects (NOEs) to reveal global features for the conformation of micelle-bound melittin. Proton-detected NMR experiments usually require the use of deuterated detergents. Heteronuclear NMR experiments can help in eliminating the interference of detergent signals through the intrinsic filtering effects of the pulse sequence. It has been suggested that for large membrane protein-detergent complexes there is no significant difference in the quality of heteronuclear correlation spectra obtained using a nondeuterated or perdeuterated detergent [54]. For example, the quality of [^{15}N,^{1}H]-TROSY and TROSY-HNCA spectra of the 30 kDa human β-barrel outer membrane protein VDAC-1 was independent of the degree of detergent deuteration [55]. The same study, however, also showed a sensitivity decrease of around 10-30% in ^{15}N-resolved [^{1}H,^{1}H]-NOESY spectra when going from deuterated to protonated detergent and use of deuterated detergent was essential for the recording of 3D and 4D NOESY-type spectra of isoleucine, leucine and valine methyl groups [55]. It therefore appears that while backbone directed experiments may be performed in a protonated detergent, NOE experiments and experiments involving side-chain signals have clear benefits from the use of deuterated detergents. Also, the studies described above that comment on the effects of a deuterated detergent on the quality of heteronuclear correlation spectra both refer to β-barrel membrane proteins. We suggest that the effects of a deuterated detergent are protein-specific since in our experience with a large α-helical membrane protein, a deuterated detergent was essential for achieving the best quality [^{15}N,^{1}H]-TROSY spectra (see section 3.4). The use of a deuterated detergent is generally beneficial to solution-state NMR structural studies of membrane proteins [12].

Another technique for which deuterated detergents have been crucial for obtaining structural information about membrane proteins in solution is small-angle neutron scattering (SANS). Using solvent-contrast variation (H_2O/D_2O exchange), SANS is especially powerful for determining the shape, size and structural organization of membrane proteins in multi-component assemblies [56-66]. Deuteration of different sample components in SANS experiments exploits the intrinsic neutron scattering length difference between hydrogen and deuterium, which selectively targets specific regions of the sample and enhances the contrast between them [67-74]. Hydrogen and deuterium have neutron coherent scattering lengths (b_c) of −3.7423 fm and 6.675 fm, respectively, which results in very different scattering length densities (SLDs) for H_2O and deuterium oxide (D_2O) of -0.562×10^{10} cm^{-2} and 6.404×10^{10} cm^{-2}, respectively [67]. In a sample containing deuterated detergent, the signals from the detergent can be matched out in D_2O so that only signal from a solubilized membrane protein remains visible in the scattering profile, which simplifies data analysis.

Despite the essential requirement for deuterated detergents in NMR and SANS studies of membrane proteins, they are usually challenging and expensive to synthesize [12]. The amphipathic nature of detergents immediately introduces extra challenges to the synthesis of these compounds and their precursors, especially in work-up and purification steps. Introduction of partial or complete deuteration into detergent compounds requires identification of suitable and commercially available deuterated starting compounds and/or reagents along with an appropriate synthetic route. Furthermore, the deuterated precursor compounds are themselves generally relatively expensive since they must be produced by biological or chemical deuteration. Details for producing specific deuterated precursor compounds for synthesis of deuterated detergents are described in later sections of this article. The original source of deuterium nuclei for these deuterated precursor compounds is usually D_2O, which is produced using the Girdler-Sulphide or Girdler Spevack process that depends on exchange of deuterium atoms between molecules in a mixture of water and hydrogen sulphide [75]; this is followed by final concentration to 99.8% heavy water by vacuum distillation or electrolysis based on Nobel prize winning work by Urey and co-workers [76, 77].

It is fortunate that, chemically, deuterium behaves similarly to ordinary hydrogen, but there are significant differences in bond energy and in bond length for compounds of heavy hydrogen isotopes that are larger than the isotopic differences in any other element. For example, the C-D bond is around 10 times stronger than the C-H bond and therefore more resistant to breakage; O-D, N-D and S-D bonds are also stronger than the corresponding protonated forms [78, 79]. Such large effects are seen because when hydrogen is replaced with deuterium the mass is doubled, whilst there is a much smaller change in mass for isotope substitutions of other elements such as ^{12}C for ^{13}C or ^{14}N for ^{15}N. Consequently, deuteration can have large effects on the rates of chemical and biochemical reactions, especially when the position of deuteration is directly involved in the breaking or formation of covalent bonds in the rate limiting step (primary kinetic isotope effect) [80, 81]. Indeed, experimental kinetic isotope effect values for deuterium (= rate of reaction with protium/rate of

reaction with deuterium, kH/kD) can be as large as 10 or more with a theoretical maximum of 18 [81, 82-87], whilst experimental values for ^{13}C or ^{15}N are typically in the range 1.01-1.07 with a theoretical maximum of 1.25 [82, 86, 88, 89]. The deuterium kinetic isotope effect has been used to study reaction mechanisms, enhance the stability of technical products against oxidative and hydrolytic degradation and to alter the rates of metabolism and the pharmacokinetic effects of drug compounds [80, 86, 90-100]. Deuterium isotope effects on noncovalent interactions between molecules are generally much less significant but they can be substantial [89]. Based on some of the investigations performed so far, deuteration of proteins does not appear to have significant effects on protein structure, but it can affect protein function and substrate specificity through kinetic isotope effects [101-106]. No published work appears to be available on the effects of deuteration on detergent properties (e.g., shape, CMC, aggregation number, solubility, thermodynamic and volumetric parameters, phase behaviour) or the effects of deuterated detergents on the solubilization of proteins or on protein structure or function.

In this book chapter we provide an updated and expanded version of our earlier review article "Deuterated detergents for structural and functional studies of membrane proteins: Properties, chemical synthesis and applications" [12]. In the following sections we consider detergent screening approaches, the properties and chemical synthesis of deuterated detergents and examples of their applications for structural and functional studies of membrane proteins using solution-state NMR and SANS, and some guidelines for choosing an appropriate detergent.

2. DETERGENT SCREENING

In choosing the most suitable detergent for NMR studies with a membrane protein a number of factors must be considered [12]. These include achievement of good quality spectra or scatter plots from a stable sample under conditions that retain the native structure and activity of the protein. The detergent that provides the highest quality spectra or scatter plot is not necessarily the best for retaining structure and activity, so a balanced view must be taken. Due to curvature of the water-micelle interface detergents that form the largest micelles tend to have the least deleterious effects on membrane protein structure, but it is more challenging to achieve high resolution NMR spectra for larger complexes.

The screening of detergents for experimental studies with membrane proteins has some common attributes for using a wide range of techniques, including X-ray crystallography and other diffraction methods, cryoEM, mass spectrometry and NMR spectroscopy. An initial screen of multiple detergents can simply determine if the protein is soluble or if it precipitates. This can involve purification in a mild and stable detergent, binding to an affinity column, washing and elution with a buffer containing a new detergent and running on an SDS-PAGE gel. If the protein precipitates in the new detergent it will remain on the column or if the protein is solubilized by the new detergent it will be eluted and give a band on the gel. In this test the concentrations of both protein and detergent can be varied and it can be made high-throughput. Under conditions of successful solubilization, the protein can then be tested for structural and functional integrity, monodipersity and thermal stability using a range of enzymatic, ligand binding or spectroscopic assays of which some can be made high-throughput. Circular dichroism spectroscopy can be used to test secondary structure (far-UV) and tertiary structure (near-UV) integrity, thermal stability and ligand binding activity [107-116]. Fluorescence spectroscopy can be used to test structural integrity (spectral shape), ligand binding activity and thermal stability [117] and a microscale fluorescent screen using the thiol-specific fluorochrome *N*-[4-(7-diethylamino-4-methyl-3-coumarinyl)phenyl]maleimide (CPM) has been developed for screening stability [118]. A high-throughput detergent screening method using differential scanning fluorimetry in combination with scattering upon thermal denaturation was developed to study the unfolding of integral membrane proteins [119]. Light scattering and turbidity measurements can be used to test for aggregation and to measure particle size [120-124]. Differential filtration can be used to screen stability and particle size [125]. Electrophoresis (e.g., SDS-PAGE, native-PAGE) and chromatography (e.g., size exclusion) can be used alongside these techniques to test for structural degradation, aggregation, monodispersity and oligomerization and to measure the size of protein-detergent complexes. Analytical ultracentrifugation can be used to investigate the oligomeric state and the detergent-to-protein ratio in protein-detergent complexes and to evaluate sample homogeneity [126]. Cell-free expressed membrane proteins can be produced in the presence of a detergent, which can also serve as an initial test for solubilization or precipitation [127]. Because deuterated detergents are generally not used for crystallography, the use and screening of detergents for crystallography will not be considered further in this review and the reader is referred to other published work on this theme [5, 10, 14, 128-132].

Regardless of the techniques described above, the detergent solubilized protein will only be suitable for solution-state NMR studies if it produces sufficiently high-quality multidimensional NMR spectra in terms of sensitivity and resolution, number and dispersion of peaks and lifetime of the sample [12]. This can initially be assessed by obtaining 2D correlation ^{15}N-^{1}H HSQC or TROSY or ^{13}C-^{1}H methyl-TROSY NMR spectra for highly pure ^{15}N and/or ^{13}C-labelled protein in homogenous samples with different detergents and with varying concentrations of protein and detergent and using different temperatures, pH values and salt

concentrations [40, 133, 134]. Larger proteins will likely require deuteration of the protein and benefit from a deuterated detergent for the reasons already described. The area under the amide proton region in 1D ^{1}H spectra as a function of time can be used as an indicator of NMR sample stability [133]. The lifetime of peaks in the NMR spectra should correlate with measurements in the stability of protein structural integrity and activity obtained using other techniques under the same sample and temperature conditions. For some detergent-solubilized membrane proteins, such as receptors or those with an enzymatic function, an activity assay using the natural ligand or substrate may be feasible. For other membrane proteins, such as channels and transporters, an assay of their functional activity is not usually possible under detergent solubilized conditions, so an assay of inhibitor binding may be used. In some cases membrane protein activity may be demonstrated in an NMR experiment by observing the shift, appearance or disappearance of peaks following addition of an appropriate ligand. The size of membrane protein-detergent complexes in the NMR sample can be estimated from pulsed field gradient (PFG) translational diffusion measurements [133, 135, 136] or from rotational correlation times obtained using NMR relaxation measurements [133, 137, 138]. For membrane proteins available only in small quantities, microcoil NMR technology has been developed for screening the detergent solubilization, proper folding and translational diffusion of microscale quantities of membrane proteins destined for structural studies [139-142]. There have been some attempts to rationalize the predictive selection of detergents for optimal solubilization, sample homogeneity and native protein folding with specific membrane proteins in NMR structural studies. These include the design of mixed micelles based on matching of micelle dimensions to those of the hydrophobic surface of the protein to avoid exchange processes that reduce NMR observations [143], correlation of micelle properties with ligand-binding activity [144], assessment of amino acid sequence hydropathy [145] and the effects of detergent concentration and changes in effective CMC values for specific detergents in the presence of a membrane protein [141]. Clearly, more work on this theme must be performed before robust generalized guidelines can be made for predictive detergent selection.

3. DEUTERATED DETERGENTS

The use of deuterated detergents in experimental studies with membrane proteins using solution-state NMR and SANS introduces extra considerations, which include the pattern of deuteration in the detergent molecule, availability and cost [12]. The most commonly used detergents that are currently commercially available in deuterated forms are listed as follows: sodium dodecyl sulphate (SDS) in perdeuterated form (d_{25}-SDS); lauryldimethylamine-oxide (LDAO) in perdeuterated form (d_{31}-LDAO); *n*-octyl-β-*D*-glucoside (β-OG) with the aliphatic tail deuterated (d_{17}-β-OG) and in perdeuterated form (d_{24}-β-OG); *n*-dodecyl-β-*D*-maltoside (DDM) with the aliphatic tail deuterated (d_{25}-DDM); fos-choline-10 (*n*-decylphosphocholine) with a semi-deuterated head (d_9-fos-choline-10), with a perdeuterated head (d_{13}-fos-choline-10) and in perdeuterated form (d_{34}-fos-choline-10); fos-choline-11 (*n*-undecylphosphocholine) with a semi-deuterated head (d_9-fos-choline-11) and with a perdeuterated head (d_{13}-fos-choline-11); fos-choline-12 (dodecylphosphocholine, DPC) with a semideuterated head (d_9-DPC), perdeuterated head (d_{13}-DPC), tail deuterated (d_{25}-DPC) and in perdeuterated form (d_{38}-DPC); fos-choline-14 (*n*-tetradecylphosphocholine) with a semideuterated head (d_9-fos-choline-14), perdeuterated head (d_{13}-fos-choline-14) and in perdeuterated form (d_{42}-fos-choline-14). The chemical structures of these detergents are shown in Figure 1A and some of their properties are given in Table 1.

Table 1: Properties of detergents. These properties are for the undeuterated compounds and were obtained from catalogues of the product suppliers: Anatrace, Cambridge Isotope Laboratories, Cortecnet, Generon, Sigma-Aldrich

	SDS	LDAO	β-OG	DDM	Fos-choline-10	Fos-choline-11	Fos-choline-12	Fos-choline-14
Detergent type	Anionic	Zwitterionic	Non-ionic	Non-ionic	Zwitterionic	Zwitterionic	Zwitterionic	Zwitterionic
Aliphatic chain length	12xC	12xC	8xC	12xC	10xC	11xC	12xC	14xC
Molecular formula	$C_{12}H_{25}SO_4Na$	$C_{14}H_{31}NO$	$C_{14}H_{28}O_6$	$C_{24}H_{46}O_{11}$	$C_{15}H_{34}NO_4P$	$C_{16}H_{36}NO_4P$	$C_{17}H_{38}NO_4P$	$C_{19}H_{42}NO_4P$
Molecular weight	288.4	229.4	292.4	510.6	323.4	337.4	351.5	379.5
Melting point	206 °C	132-133 °C	98-103 °C	224-226 °C	93-96 °C	93-96 °C	93-96 °C	93-96 °C
CMC[a]	6-8 mM	1-2 mM	20-25 mM	0.2 mM	11 mM	1.9 mM	1.5 mM	0.12 mM
Aggregation number[a]	62	76	84	98	24	18	54	108
Micelle molecular weight	18 kDa	17.5 kDa	25 kDa	50 kDa	7.8 kDa	6 kDa	19 kDa	47 kDa
Solubility[a]	0.1 M	≥30%	>1 g in 10 ml	≥20%	≥10%	≥20%	≥20%	≥10%

[a]In H_2O at 20 °C

3.1. Sodium Dodecylsulphate

Sodium dodecylsulphate (SDS), also known as sodium lauryl sulphate, is an anionic detergent with an aliphatic 12-carbon chain and a small negatively charged head group (Table 1 and Figure 1A). SDS is a harsh detergent often used as a protein denaturant, hence its use in polyacrylamide gel electrophoresis for the separation of proteins and for estimation of their molecular masses in a denatured state. Despite these properties, SDS has been used to solubilize a significant number of membrane proteins for investigations of their structure and function [12]. In the case of solution-state NMR, the

principal reason for this is its ability to form relatively small and uniform complexes with membrane proteins that tumble fast enough in solution to achieve high-resolution spectra. The large majority of NMR structures determined in SDS micelles are for membrane peptides or for relatively small α-helical membrane proteins. Structures of membrane proteins determined in SDS micelles include fd coat protein [146], the mitochondrial membrane protein stannin [147], MerF of the mercury detoxification system from *Morganella morganii* [148], the human zetazeta-transmembrane domain [149], a thermostable mutant of the potassium ion channel KcsA [150], the human DAP12-NKG2C heterotrimeric immunoreceptor complex [151], LC4 region of CC chemokine receptor 5 [152] and regulatory subunits of the the Na,K-ATPase [153-155].

The synthesis of SDS is usually achieved by sulphonation of *n*-dodecanol [156] using sulphur trioxide [157], chlorosulphonic acid [158] or sulphuric acid [159] followed by neutralization of the resultant sulphate using sodium hydroxide or sodium carbonate (Figure 2A). Uniformly deuterated SDS (d_{25}-SDS) can be produced by using d_{25}-*n*-dodecanol in this synthesis. d_{25}-*n*-Dodecanol, which is commercially available, can be produced by reduction of the deuterated fatty acid (d_{23}-*n*-dodecanoic acid) using lithium aluminium deuteride ($LiAlD_4$). An early method for preparing saturated fatty acids with deuteration at all carbon positions was to heat fatty acids with D_2O in the presence of alkali (KOH) and active platinum [160], but this method gave only partial deuteration at each position. A simple and efficient method for preparing fully deuterated fatty acids was later developed by heating (195 °C) fatty acids and deuterium gas over a palladium on charcoal catalyst [161]. High isotopic purity deuterium gas (>99.98%) can be produced by electrolysing high isotopic purity D_2O (99.8%) down to around 30% of its original volume [162]. A similar approach has been used for deuteration of fatty acyl chains in synthetic phospholipid molecules [163]. There was also a renewed and increased interest in using a variety of hydrogen/deuterium-exchange reactions at carbon centres for production of deuterium-labelled compounds rather than using classical synthesis with deuterated precursors [164]. Due to its relative ease of synthesis and longstanding commercial availability, d_{25}-SDS has been one of the most commonly used deuterated detergents for solubilising membrane proteins, principally for solution-state NMR measurements of structure, dynamics and ligand binding interactions [12].

Early NMR studies with the ion channel-forming pentadecapeptide gramicidin A achieved high-resolution 2D spectra for the peptide solubilized in d_{25}-SDS micelles. These were used to confirm that the ion-channel state of gramicidin A adopts an N-terminal to N-terminal (head-to-head) dimer formed by two right-handed, single-stranded helices with 6.3 residues per turn [165, 166]. This work also demonstrated the future potential for investigating the structure and function of ion channels solubilized in detergent micelles using solution-state NMR spectroscopy. Gramicidin A solubilized in d_{25}-SDS micelles was later used as a simplified model for transmembrane ion channels to investigate their interactions with the anaesthetic and non-immobilizer compounds 1-chloro-1,2,2-trifluorocyclobutane and 1,2-dichlorohexafluoro-cyclobutane, respectively, by 2D ^{1}H-^{1}H NOESY measurements [167]. The former compound significantly altered the chemical shifts of tryptophan indole N-H protons near the channel entrance, consistent with anaesthetic compounds causing a functional change of the channel by interacting with the amphipathic domains at the peptide-lipid water interface. Another model membrane protein, the 50-residue M13 coat protein, which becomes an integral membrane protein during the infection stage of the life cycle of the M13 phage, was solubilized in d_{25}-SDS micelles for measurement of side-chain dynamics by ^{1}H NMR [168]. ^{1}H-exchange rates for a primary amide in the side chain of glutamine-15 and for the indole amine of tryptophan-26 were measured. Whilst the glutamine-15 proton exchanged at a rate identical with that in glutamine model peptides, the tryptophan-26 indole amine proton exchange was biphasic, possibly reflecting protein dimerization or aggregation in the SDS micelles. ^{1}H NMR measurements on a model transmembrane helix based on the GCN4 leucine zipper solubilized in d_{25}-SDS micelles helped to demonstrate how inter-helical hydrogen bonding drives strong interactions in membrane proteins [169]. This was achieved by monitoring cross peaks in NOESY spectra that revealed information about an asparagine side chain and helical secondary structure near that position. Several complementary NMR approaches were used to investigate the structure and interaction of mastoparan, a 14-residue peptide toxin from wasp venom, with lipid membranes [170]. These included determination of the 3D structure of mastoparan solubilized in d_{25}-SDS using ^{1}H NOE measurements and distance geometry calculation, which revealed a straight amphipathic α-helix. Combined with solid-state NMR experiments that described the interaction, orientation and insertion of mastoparan with lipid bilayers, the results were used to propose a pore-forming peptide that can undergo a flip-flop between monolayers and therefore movement of mastoparan across the membrane. The conformation of orexin-B, an orphan G-protein coupled receptor agonist and neuropeptide implicated in sleep-wakefulness and feeding regulation, in d_{25}-SDS micelles was determined by 2D NMR and molecular modelling [171]. The 28-residue peptide had a secondary structure containing two α-helical segments (residues 7-18 and 22-26) believed to be involved in membrane binding and the unstructured C-terminus (residues 27 and 28) is proposed to have conformational freedom for binding to the receptor. Interaction of the neurotransmitters dopamine and acetylcholine with an amphiphilic resorcinarene receptor solubilized in d_{25}-SDS micelles was also investigated by

^{1}H NMR measurements [172]. Distances of these neurotransmitters from the hydrophilic cavity of the receptor were estimated based on calculation of the ring current shift using atomic coordinates obtained from molecular dynamics calculation. NMR analysis of an 18-residue amphipathic peptide (residues 392-409, also known as helix A) solubilized in d_{25}-SDS helped to demonstrate how it controls the multiple roles of the brome mosaic virus protein 1a in RNA replication complex assembly and function [173]. This study included determination of the 3D structure of the peptide based on measurement of NOE restraints and additional dihedral angle constraints, which revealed an α-helical conformation for residues 397-406 (Figure 2B). Screening of detergents for NMR analysis of the catalytic C-terminal domain (residues 466-718) of the Stt3p subunit from yeast oligosaccharyl transferase identified d_{25}-SDS to be the most suitable (over DDM, DPC, digitonin, LDAO and OG) since it produced a 2D [^{15}N-^{1}H]HSQC spectrum with good dispersion and narrow line widths providing a count of 245 resolved peaks out of 263 non-proline residues [174]. Furthermore, CD spectra showed that the C-terminus of Stt3p is highly helical and has a stable tertiary structure in SDS micelles. Although this work did not yet determine the structure of the Stt3p C-terminal domain, peptide ligand binding was measured using NMR saturation transfer difference (STD) and titration experiments with Ile/Leu/Val-methyl protonated samples and 2D [^{15}N-^{1}H]HSQC spectra, respectively. A structure of a 25-residue sequence (residues 623-647) from the C-terminal domain of the Frizzled receptor 1 in d_{25}-SDS micelles was determined from 104 NOE restraints (Figure 2C) [175]. This revealed that residues 627-639 formed an α-helix and that the C-terminus of the peptide was not structured. The NMR structure and an analysis of the helices hydrophobic properties indicated that it is an amphipathic α-helix, which may have similar function to the helix 8 of classical G protein-coupled receptors at the membrane interface.

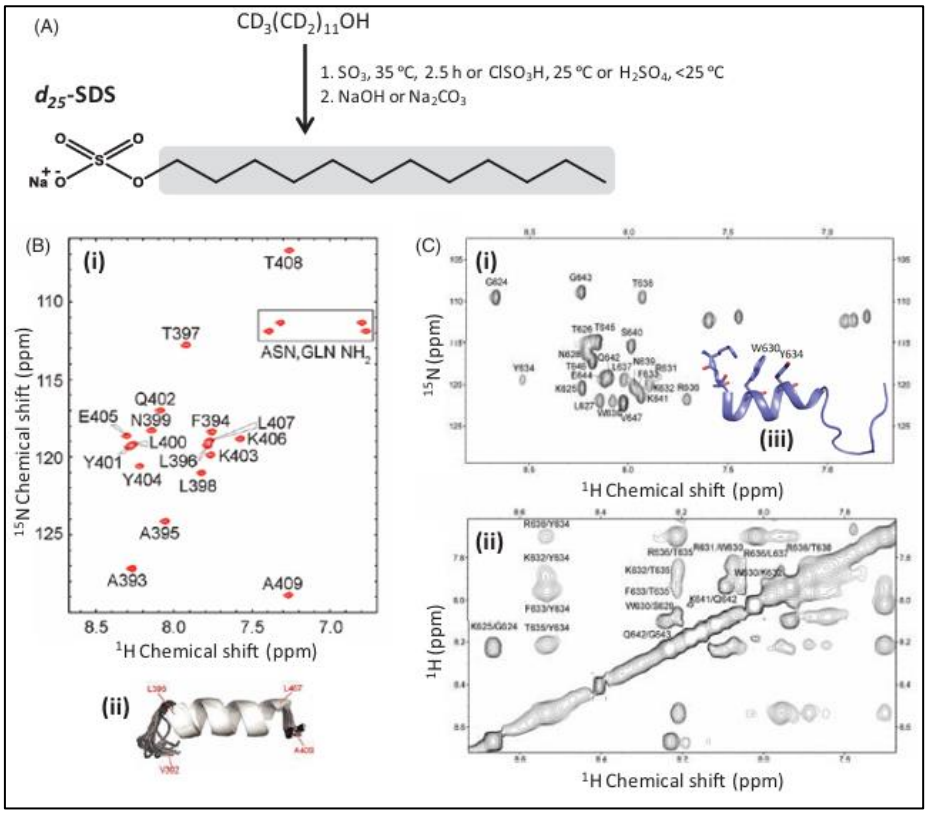

Figure 2: Synthesis of d_{25}-SDS and its use in solubilizing helix A from brome mosaic virus protein 1a and the C-terminal region of the Frizzled receptor 1. A. Synthesis of d_{25}-SDS from d_{25}-*n*-dodecanol. The grey area shows the region of deuteration. B. (i) [^{15}N-^{1}H]HSQC spectrum with assignments of brome mosaic virus 1a helix A bound to 100 mM d_{25}-SDS micelles and (ii) ensemble of 20 structures (backbone atoms only) determined for helix A bound to an SDS micelle where white = helix and grey = coil. C. (i) [^{15}N-^{1}H]HSQC spectrum with assignments of the C-terminal region of the Frizzled receptor 1 (residues 623-647) in d_{25}-SDS micelles, (ii) NOESY spectrum with NOE interactions labelled and (iii) structure determined from 104 NOE restraints. This Figure was reproduced from Hiruma-Shimizu *et al.,* (2015) [12].

In addition to NMR, d_{25}-SDS has also been used in SANS studies with membrane proteins as a contrasting reagent, especially for investigation of association states and conformational changes [12, 57]. For example, SANS contributed to a study of the multimeric forms of the small multidrug resistance protein EmrE solubilized in d_{25}-SDS micelles revealing different shapes for EmrE at varying concentrations of detergent and in presence of the substrate tetraphenyl phosphonium [176]. In these experiments the use of d_{25}-SDS instead of hydrogenated

SDS enhanced the contrast for EmrE within the detergent micelle. The water solvent was contrast-matched with d_{25}-SDS so that the detergent became invisible due to the differences in deuterium/hydrogen scattering angles and resulting in the scattering pattern being that of EmrE alone.

3.2. Lauryldimethylamine-Oxide

Lauryldimethylamine-oxide (LDAO), also known as *N*,*N*-dimethyldodecylamine-*N*-oxide (DDAO), is a non-denaturing zwitterionic detergent with an aliphatic 12-carbon chain (Table 1 and Figure 1A). LDAO has been used to solubilize a small number of membrane proteins for determination of their 3D structure by solution-state NMR [12]. These proteins include the autonomously folding *Bacillus subtilis* protein mistic that can be used for high-level production of other membrane proteins [177], the human voltage-dependent anion channel (VDAC-1) [55, 178, 179] and transmembrane domains of the α4 and β2 subunits of the nicotinic acetylcholine receptor [180]. Uniformly deuterated LDAO (d_{31}-LDAO) is commercially available from several sources and a synthesis from d_{23}-dodecanoic acid has been described [181]. D_{23}-Dodecanoic acid was reacted with d_6-dimethylamine to give d_{29}-*N*,*N*-dimethyldodecanoylamide, which was reduced to the amine using d_4-lithium aluminium hydride then oxidation with hydrogen peroxide gave d_{31}-LDAO (Figure 3A).

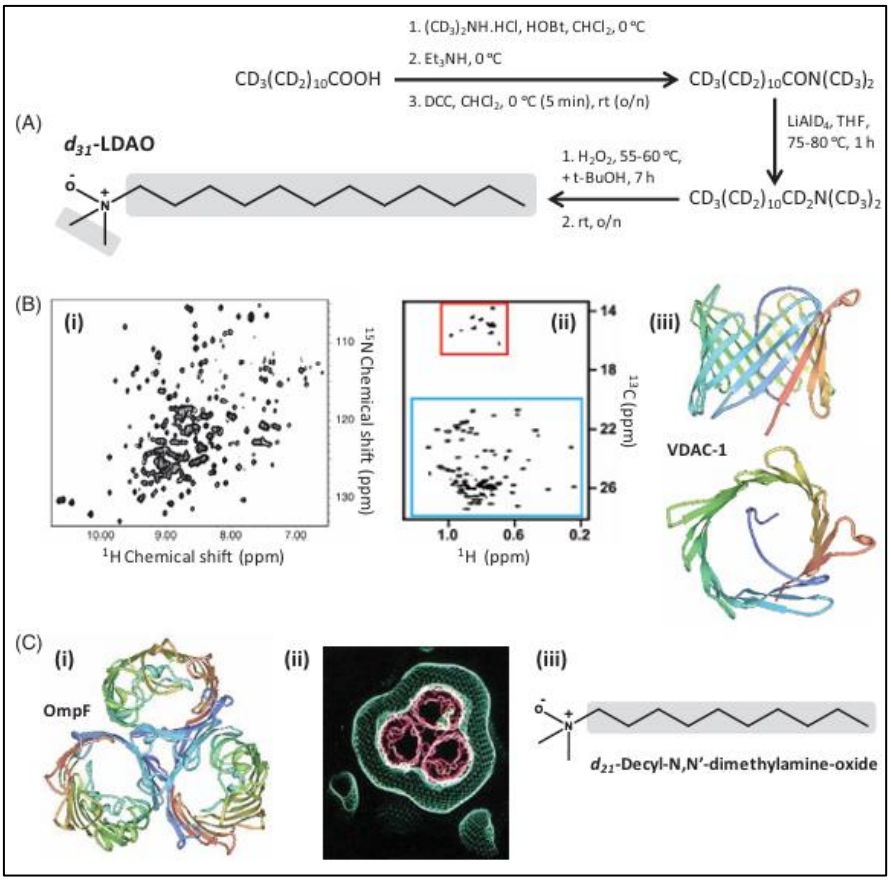

Figure 3: Synthesis of d_{31}-LDAO and its use in solubilizing the human voltage-dependent anion channel (VDAC-1) and use of tail-deuterated decyl-*N*,*N*$_0$-dimethyl amine oxide in solubilizing *E. coli* outer membrane protein OmpF. A. Synthesis of d_{31}-LDAO from d_{23}-dodecanoic acid. The grey areas show the regions of deuteration. B. (i) [^{15}N-^{1}H]-TROSY spectrum of [U-^{2}H,^{15}N]VDAC-1 in d_{31}-LDAO micelles, (ii) [^{13}C-^{1}H]HMQC spectrum of [U-^{2}H,^{13}C,^{15}N; 1Hd-IL; 1Hg-V]VDAC-1 in d_{31}-LDAO micelles highlighting the spectral regions for Ile residues (red box, 11/11 assigned) and Leu plus Val residues (blue box, 8/12 Val and 17/28 Leu assigned), (iii) structure of human VDAC-1 shown as a side view (top) and from above (bottom) with the N-terminus in blue and C-terminus in red, which were drawn using PDB file 2K4T and PDB Protein Workshop 3.9 [188]. C. (i) Crystal structure of the *E. coli* outer membrane protein OmpF in tetragonal crystal form as an above view with the N-terminus in blue and C-terminus in red, which was drawn using PDB file 1OPF and PDB Protein Workshop 3.9 [188]. (ii) Single-crystal neutron diffraction density map of OmpF in tail-deuterated decyl-*N*,*N*$_0$-dimethyl amine oxide detergent contrast mapped parallel to the three-fold trimer axis where the porin trimer is represented by the Cα trace (pink) obtained from the X-ray crystal structure. (iii) Structure of the detergent d_{21}-decyl-*N*,*N*$_0$-dimethyl amine oxide. The grey area shows the region of deuteration. This Figure was reproduced from Hiruma-Shimizu *et al.*, (2015) [12].

The same work also used the d_{31}-LDAO and ^{2}H solid-state NMR to investigate phase equilibria and molecular packing in a system of LDAO/peptide gramicidin D/water [181]. The deuterated precursor compound d_{23}-dodecanoic acid is commercially available and its production by deuteration of the

unlabelled fatty acid was described in the section for SDS. D_6-Dimethylamine can be prepared from d_9-trimethylamine via d_9-trimethylamine-*N* oxide [182] and the d_9-trimethylamine can be prepared by heating deuterated methyl iodide (CD_3I) and ammonium hydroxide (NH_4OH) [183]. The d_4-lithium aluminium hydride ($LiAlD_4$) can be prepared from lithium deuteride (LiD) and aluminium bromide ($AlBr_3$) with prior preparation of lithium deuteride by the direct combination of lithium and deuterium at 700 °C with the deuterium having been obtained from D_2O using magnesium [184]. The solution-state NMR structure determination of human VDAC-1 used d_{31}-LDAO for solubilization revealing a novel β-barrel fold with 19 transmembrane strands and with the first and last strands parallel with each other giving a closed structure (Figure 3B) [179]. The NMR structure of human VDAC-1 was in close agreement with a combined NMR/X-ray crystal structure of the same protein [178] and with an X-ray crystal structure of mouse VDAC-1 [55, 185].

A tail-deuterated form a of a related detergent decyl-*N*,*N*-dimethyl amine oxide has been used in single-crystal neutron diffraction studies with the *E. coli* outer membrane protein OmpF in its tetragonal crystal form [12, 186]. In the tetragonal crystal form of OmpF the protein surface normally buried in the membrane is accessible to the detergent solution and therefore provides an opportunity for protein-detergent interactions to be studied. Using the X-ray crystal structure [187] as a model, the neutron diffraction measurements revealed how detergent molecules bind to the hydrophobic region of the OmpF trimer that is exposed to lipid in its native environment (Figure 3C). These measurements used partially deuterated decyl-*N*,*N*-dimethyl amine oxide to increase the contrast between protein and detergent [186].

3.3. *n*-Octyl-β-*D*-glucoside

n-Octyl-β-*D*-glucoside (β-OG) is a non-ionic detergent with an aliphatic eight-carbon chain (Table 1 and Figure 1A). The mild and non-denaturing properties of β-OG make it an attractive detergent to solubilize membrane proteins for studies of their structure and function, but its shorter chain length can contribute to protein deactivation. Only a few NMR structures of membrane proteins have been determined in β-OG micelles, presumably because the shorter aliphatic chain does not usually produce the most stable sample and/or best quality spectra compared with the longer chain detergents [12]. β-OG is commercially available with just the aliphatic chain deuterated (d_{17}-β-OG) and in perdeuterated form (d_{24}-β-OG), which can be synthesized by coupling *n*-octanol with *D*-glucose using one or both of these starting compounds in their deuterated forms, respectively [189, 190] (Figure 4A). The deuterated precursor compound d_{17}-*n*-octanol is commercially available and can be produced by reduction of the deuterated fatty acid d_{15}-*n*-octanoic acid with deuterated lithium aluminium hydride ($LiAlD_4$); the deuteration of fatty acids was described in the section for SDS. The d_7-*D*-glucose is commercially available and can be isolated from the hydrolysate of the carbohydrate fraction of algae grown in a deuterated medium or prepared using an isotopic hydrogen-exchange technique that introduces deuterium by catalytic exchange with carbon-bound hydrogen. The exchange reaction uses D_2O and deuterated Raney nickel, which itself is produced using D_2O [191]. A synthesis of β-OG, and of other sugar-containing detergents, using a microwave-assisted glycosylation reaction from methyl glycosides may be useful for improving the yields of the deuterated compounds [192]. The best-known NMR structure for a membrane protein solubilized in d_{24}-β-OG micelles is that for the bacterial outer membrane enzyme PagP, which transfers a palmitate chain from a phospholipid to lipid A [193]. The structure, which was also determined in d_{38}-DPC micelles, consists of an eight-stranded anti-parallel β-barrel preceded by an N-terminal amphipathic α-helix (Figure 4B).

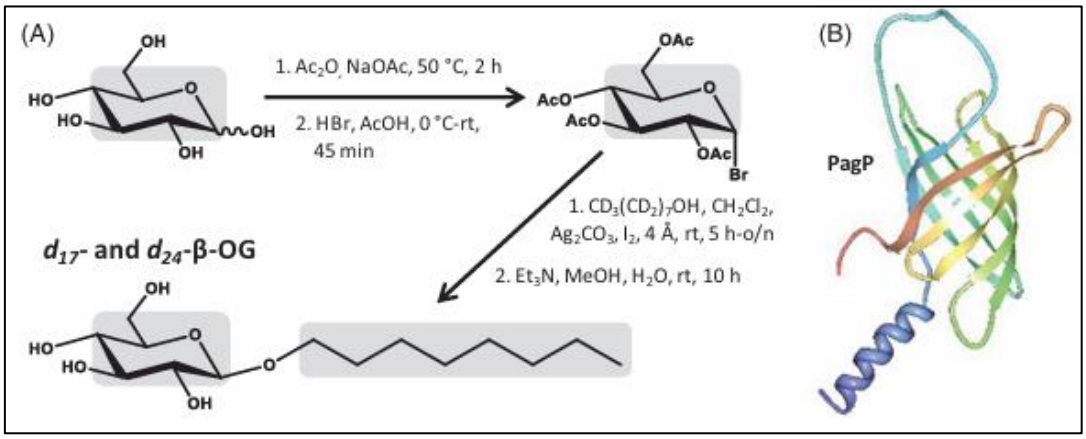

Figure 4: Synthesis of d_{17}- and d_{24}-β-OG and use of d_{24}-β-OG in solubilizing the bacterial outer membrane enzyme PagP. A. Synthesis of d_{17}- and d_{24}-β-OG from d_{17}-*n*-octanol and d_7-*D*-glucose. The grey areas show the regions of deuteration. B. Structure of PagP with the N-terminus in blue and C-terminus in red, which was drawn using PDB file 1MM5 and PDB Protein Workshop 3.9 [188]. This Figure was reproduced from Hiruma-Shimizu *et al.,* (2015) [12].

Deuterated forms of β-OG have also been used for solubilization of membrane proteins in SANS experiments [12, 57], including d_{17}-β-OG with the outer-membrane 16-stranded β-barrel transport protein FhaC of the *Bordetella pertussis* filamentous hemagglutinin adhesion [194]. SANS measurements were combined with molecular modelling to describe the solution structure of FhaC in which the N-terminal α-helix was inside the pore consistent with the crystal structure [195].

In a study that demonstrated how detergents can be made "invisible" in SANS determination of membrane protein structure, a novel method for synthesising β-OG allowed for selective deuteration at different predetermined levels at its head and tail groups so that they were fully matched out in D_2O buffer. The theoretical level of deuteration needed for β-OG to be matched-out in 100% D_2O was a ratio of D7.6/H3.4 in the head group and D15.9/H1.1 in the tail group [196]. In this method, the partial specific molecular volumes of the head and tail groups were determined by densitometry. The multiple step synthesis firstly involved deuterating the alkyl chain of *n*-octanoic acid at the required deuteration level using a hydrothermal Pt/C catalysed H/D exchange reaction at 220 °C in the appropriate molar ratio of deuterium and hydrogen atoms in the mixture, which reduced it to *n*-octanol. The deuterated *n*-octanol was coupled to 2,3,4,6-tetra-*O*-acetyl-α-*D*-glucopyranosyl bromide (Ag_2CO_3/$AgClO_4$/Molecular Sieves 4 Å), followed by deacetylation of the sugar head group (NaOMe). The required level of deuteration in the sugar head was then achieved by using mild conditions of Raney Nickel catalyst in a D_2O/H_2O mixture at 80 °C for 18 h. This last step incorporated deuterium atoms on the four carbons adjacent to free hydroxyl groups (α positions) in the sugar head group with retention of configuration. The membrane protein of interest was initially purified in hydrogenated buffer and hydrogenated detergent, then a size exclusion purification was performed in the equivalent deuterated buffer and matched-out deuterated detergent. The feasibility of using the custom-synthesized matched-out deuterated β-OG in SANS studies was demonstrated on five different membrane proteins: bacteriorhodopsin (bR) (~27 kDa), photosystem I (PSI) (~650 kDa), maltoporin (LamB) (~47 kDa), ionotropic glutamate receptor A2 (GluA2) (~385 kDa), sarco/endoplasmic reticulum Ca^{2+} ATPase (SERCA) (~110 kDa) [196].

In a different study, a mixture of 54.6% fully deuterated, 36.4% tail-deuterated and 8.9% non-deuterated β-OG (mole percentages) enabled the detergent to matched-out in 100% D_2O buffer in SANS experiments that investigated the distribution of bacteriorhodopsin and detergent in the lipidic cubic phase [197].

3.4. *n*-Dodecyl-β-*D*-maltoside

n-Dodecyl-β-*D*-maltoside (DDM) is a non-ionic detergent with an aliphatic 12-carbon chain (Table 1 and Figure 1A), which tends to disrupt lipid-lipid and lipid-protein interactions but not protein-protein interactions. The mild and non-denaturing properties of DDM make it a commonly used detergent for the extraction and purification of membrane proteins and for solubilization in experimental studies of their structure, dynamics and function [4, 7, 12, 109, 113, 114, 115, 116, 198-202]. DDM tends to retain the native structure and functional activity of membrane proteins to a greater extent than any other detergents [118]. It can therefore serve as the control condition when screening different detergents for structural and functional studies of membrane proteins and can be used to validate the use of other detergents. Despite being one of the most successful detergents for membrane protein crystallization [203-205], relatively few NMR studies of membrane proteins have been performed using DDM, however, since it tends to form relatively large protein-micelle complexes compared with those of other detergents [12]. Solution-state NMR studies using DDM include work with the potassium ion channel KcsA [206, 207], a model polytopic α-helical membrane protein TM0026 from the thermophile *Thermotoga maritima* [143], the human β2-adrenoreceptor (β_2AR) [208], *E. coli* sugar transport protein GalP [117], the human peripheral myelin protein 22 (PMP22) [209] and the human A_2A adenosine receptor [210].

DDM with deuteration in just the aliphatic chain (d_{25}-DDM) is commercially available, but a perdeuterated form (d_{39}-DDM) is not. d_{25}-DDM can be synthesized by coupling maltose with d_{25}-*n*-dodecanol (Figure 5A) [211, 212] and this has been used in solution-state NMR studies with bacteriorhodopsin [213, 214] and with the potassium ion channel KcsA [215]. It has also been used in investigations of the composition of supported model membranes determined by neutron reflection [212, 216], in studies of hydrogen oxidation by a membrane-bound hydrogenase immobilized on gold electrodes [217] and in SANS studies of solubilized membrane proteins [57].

The first synthesis of d_{39}-DDM was reported in 2014 [12, 218]. This first required the coupling of two molecules of d_7-*D*-glucose with an α(1→4) glycosidic bond to give d_{14}-maltose followed by coupling with d_{25}-*n*-dodecanol to give d_{39}-DDM (Figure 5A). Methods for preparing the deuterated precursor compounds d_{25}-*n*-dodecanol and d_7-*D*-glucose were described in the sections for SDS and β-OG, respectively. The synthesized d_{39}-DDM was used to solubilize the 52 kDa *E. coli* sugar transport protein GalP to achieve the best resolution and highest sensitivity [^{15}N-^{1}H]TROSY spectra for amino acid selective labelled samples of a membrane protein with 12 unique transmembrane-spanning a-helices (Figure 5B) [12, 117]. Based on the costs of the synthesis, the cost of d_{39}-DDM per typical

NMR sample at the time was £500-£1000. This work also achieved high resolution [^{13}C-^{1}H]methyl-TROSY spectra for ILV-selective labelled samples of GalP and used the spectra to detect binding of a small-molecule inhibitor, which was possible using non-deuterated DDM for solubilization. For performing more advanced methyl-TROSY based experiments on the largest membrane protein-detergent complexes, use of a deuterated detergent is likely to be essential, however.

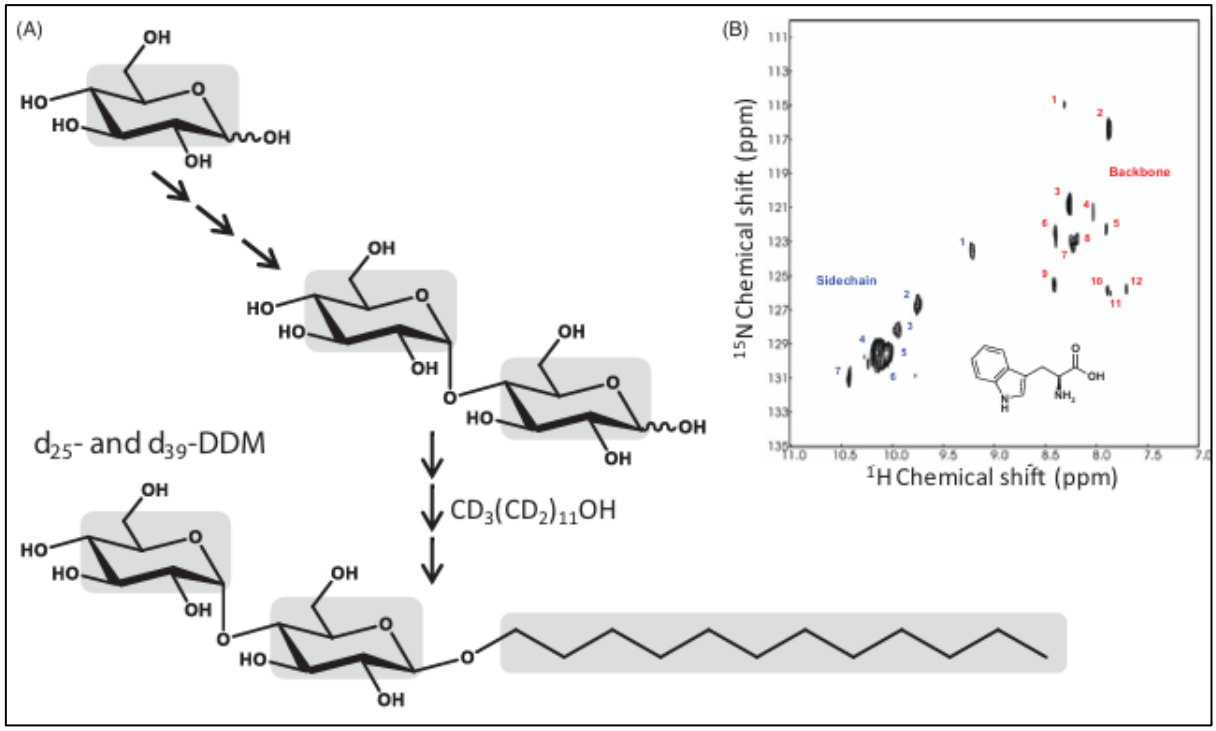

Figure 5: Synthesis of d_{25}- and d_{39}-DDM and use of d_{39}-DDM in solubilizing the *E. coli* sugar transport protein GalP. A. Synthesis of d_{25}- and d_{39}-DDM from d_{25}-*n*-dodecanol and d_7-*D*-glucose, see the work of Hiruma-Shimizu et al. (2014) [218] for the complete synthesis, reaction and experimental details. The grey areas show the regions of deuteration. B. [^{15}N-^{1}H]TROSY spectrum at 900 MHz of [U-^{2}H, $^{15}N_2$-Trp]GalP in d_{39}-DDM micelles reproduced from Kalverda *et al.*, (2014) [117]. This Figure was reproduced from Hiruma-Shimizu *et al.*, (2015) [12].

DDM with selective deuteration to make it "invisible" in SANS studies of membrane proteins was synthesized using the same method as that described for β-OG [196]. The theoretical level of deuteration needed for DDM to be matched-out in 100% D_2O was a ratio of D15.2/H5.8 in the head group and D22.4/H2.6 in the tail group. The synthesis began with *n*-dodecanoic acid, and the coupled sugar was 2,3,6,2′,3′,4′,6′-hepta-*O*-acetyl-α-*D*-maltosyl bromide. In the DDM head group there are seven hydrogen atoms at positions that can be exchanged by deuterium. In a study that used SANS to probe the solution structure of the proton-gated pentameric ligand-gated ion channel GLIC from *Gloeobacter violaceus* [219], the sample was passed directly to the neutron beam from a size exclusion chromatography column (SEC-SANS), to minimize protein aggregation. The SEC step was used to exchange the sample to D_2O buffers with matched-out selectively-deuterated DDM prepared by the method of Midtgaard et al. (2018) [196]. The approach enabled scattering curves to be measured that demonstrated slight differences in the GLIC structure between resting and activating conditions [219]. Also using a SEC-SANS setup for detergent exchange, solution structures of photosystems I and II (PSI and PSII) from *Thermosynechococcus elongatus* were determined under near physiological conditions using deuterated DDM to match-out the detergent belt surrounding the protein [220]. The DDM used here had deuteration levels of 57% and 89% in the head and tails groups, respectively, which corresponds to an SLD of 6.36×10^{-6} Å^{-2} and was matched-out in 100% D_2O. The structures obtained by SANS were compared with the cryoEM structure of PSI and the X-ray crystal structure of PSII (Figure 6).

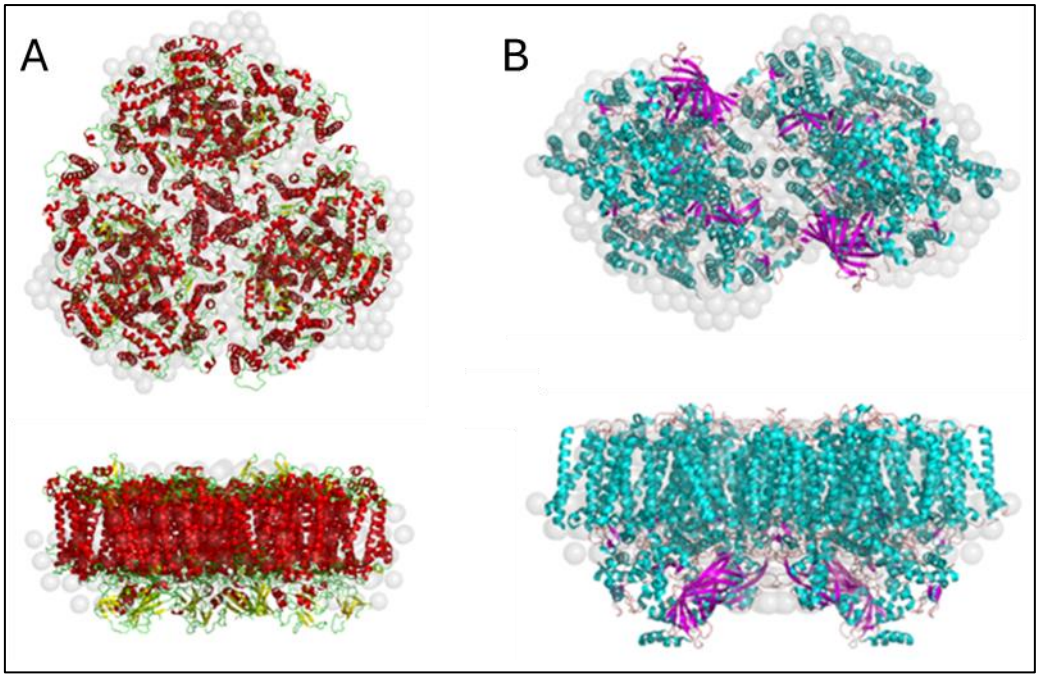

Figure 6: SANS structures of PSI and PSII SANS obtained using deuterated DDM and 100% D_2O. A. Top and side views of the PSI-dDDM complex structure reconstructed from the SANS data using the DAMMIN routine (grey spheres) superimposed to the PSI cryoEM structure (PDB 6TRD31) shown in red, yellow, and green. B. Comparison of the PSII-dDDM complex structure reconstructed from the SANS data using the DAMMIN routine (grey spheres) with the PSII crystal structure (PDB 5KAF16) shown in cyan and violet. This figure was adapted from Golub *et al.*, (2022) [220].

In SANS experiments on membrane proteins using a deuterated detergent, even if there is perfect average-contrast matching of the detergent, there can still be significant core-shell scattering from the contrast difference between hydrophilic head groups and aliphatic tail groups, which can interfere with structural data analysis [221]. To overcome this problem, a method was developed for the rational design of mixed micelles containing a deuterated detergent analogue. When contrast variation data was analysed to simulate SLDs in micelles composed of DDM only, the tail groups formed a core that was contrast-matched in 2% D_2O, while the head groups formed a shell that was contrast-matched in 49% D_2O. The overall match point for a DDM micelle was found in buffer containing ~22% D_2O. By using a mixed micelle, made by blending normal DDM and tail-deuterated DDM (d_{25}-DDM), it was possible to design a condition at which both the micelle core and shell (and therefore their average) had the same SLD at the solvent-matched condition [221]. In an example of this approach, d_{25}-DDM was used in SANS experiments to determine the solution structure of a microbial orthologue of an intramembrane aspartyl protease from *Methanoculleus marisnigri* (MmIAP). The IAP was itself deuterated and the detergent signals were fully matched-out using a specific ratio of 66% (w/v) normal DDM and 44% (w/v) d_{25}-DDM at a total concentration of 0.05% in a buffer containing 48.5% D_2O (Figure 7). From these experiments, MmIAP was determined to be a monomer [222]. A combined SANS and Martini coarse-grained molecular dynamics simulation study was used to investigate the structure and dynamics of the central lipid pool and proteins of the bacterial holo-translocon (HTL). For the SANS experiments, the HTL was solubilized in DDM that was deuterated separately in the head and tail groups so that it was completely matched out in a 100% D_2O-based buffer [223].

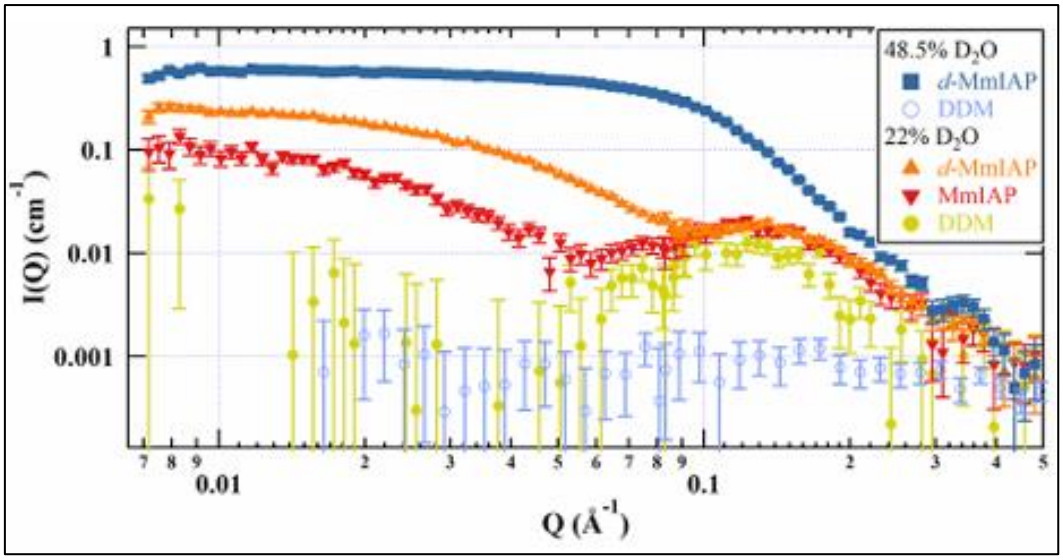

Figure 7: SANS contrast match point measurements for DDM micelles (yellow, ●), MmIAP with DDM (red, ▼), d-MmIAP with DDM (orange, ▲) in 22% D_2O, and mixed micelles (blue, ○) or d-MmIAP with DDM/d_{25}-DDM mixed micelles (blue, ■) in 48.5% D_2O. This figure was reproduced from Naing *et al.,* (2018) [222].

3.5. FOS-Cholines

The fos-cholines are zwitterionic detergents with a range in lengths of their aliphatic carbon chain (Table 1 and Figure 1A). By far the most used of these is fos-choline-12, also known as dodecylphosphocholine or DPC, which has a 12-carbon aliphatic chain. DPC is also one of the most used of all detergents [12], notably it has been used to solubilize many membrane proteins for determination of their structures by solution-state NMR [48]. An assessment of the prevalence of detergent types in membrane structural biology revealed that approximately 40% of 115 membrane protein structures determined by NMR were prepared in DPC [49, 50]. These structures include the bacterial outer membrane proteins OmpA [224, 225], PagP [193], OmpG [226], OmpX [227] and Opa60 [228], the α-helical proteins human phospholamban [229], KcsA-charybdotoxin complex [230], disulfide bond formation protein B (DsbB) [231], diacylglycerol kinase (DAGK) [232], voltage sensor domain from KvaP [233], p7 channel from hepatitis C virus [234, 235], mitochondrial uncoupling protein 2 [236] and others [42, 48]. A mention of all structures is beyond the scope of this review, but a full list of NMR structures of membrane proteins determined in DPC micelles (up to the end of 2014) is given in the Supplementary Information (Table S1) of reference 12 (available online) and others up to 2018 can be found at https://www.loquetlab.org/nmr_mpstruc/.

Approximately a half of these NMR membrane protein structures used perdeuterated DPC (d_{38}-DPC), which is commercially available and can be synthesized from d_{25}-*n*-dodecanol, d_4-ethylene glycol and d_9-trimethylamine (Figure 8A) [237]. The first reported synthesis of d_{38}-DPC used a similar approach but began with the production of deuterated *n*-dodecanol from dodecanoic acid [52]. DPC is also commercially available with a semi-deuterated head (d_9-DPC), a perdeuterated head (d_{13}-DPC) and with just the aliphatic chain deuterated (d_{25}-DPC), which are obtainable by using just one or two of the deuterated starting compounds or reagents in the synthesis. Methods for preparing the deuterated precursor compounds d_{25}-*n*-dodecanol and d_9-trimethylamine were described in the sections for SDS and LDAO, respectively. d_4-Ethylene glycol ($HOCD_2CD_2OH$) can be produced by catalytic oxidation of d_4-ethylene (CD_2CD_2) by atmospheric oxygen at 200-300 °C over a catalyst containing metallic silver to give d_4-ethylene oxide followed by hydration. The d_4-ethylene can be produced by the action of zinc dust suspended in dioxane on d_4-dibromoethane ($BrCD_2CD_2Br$), which is prepared from d_2-acetylene (CDCD) and deuterium bromide (DBr) [238]. d_2-Acetylene can be prepared from 1,4-dioxane and D_2O and DBr prepared by the action of D_2O on redistilled phosphorus tribromide [238]. The Fos-cholines with other chain lengths can be produced in deuterated forms by using the appropriate deuterated alcohol in the synthesis (Figure 8A). One of the first NMR structures of a β-barrel membrane protein, the transmembrane domain of OmpA, was determined with the protein solubilized in d_{38}-DPC micelles to reveal an eight-stranded antiparallel β-barrel (Figure 8B) [224] that was closely similar to a crystal structure of the same protein in *n*-octyltetraoxyethylene micelles [239, 240].

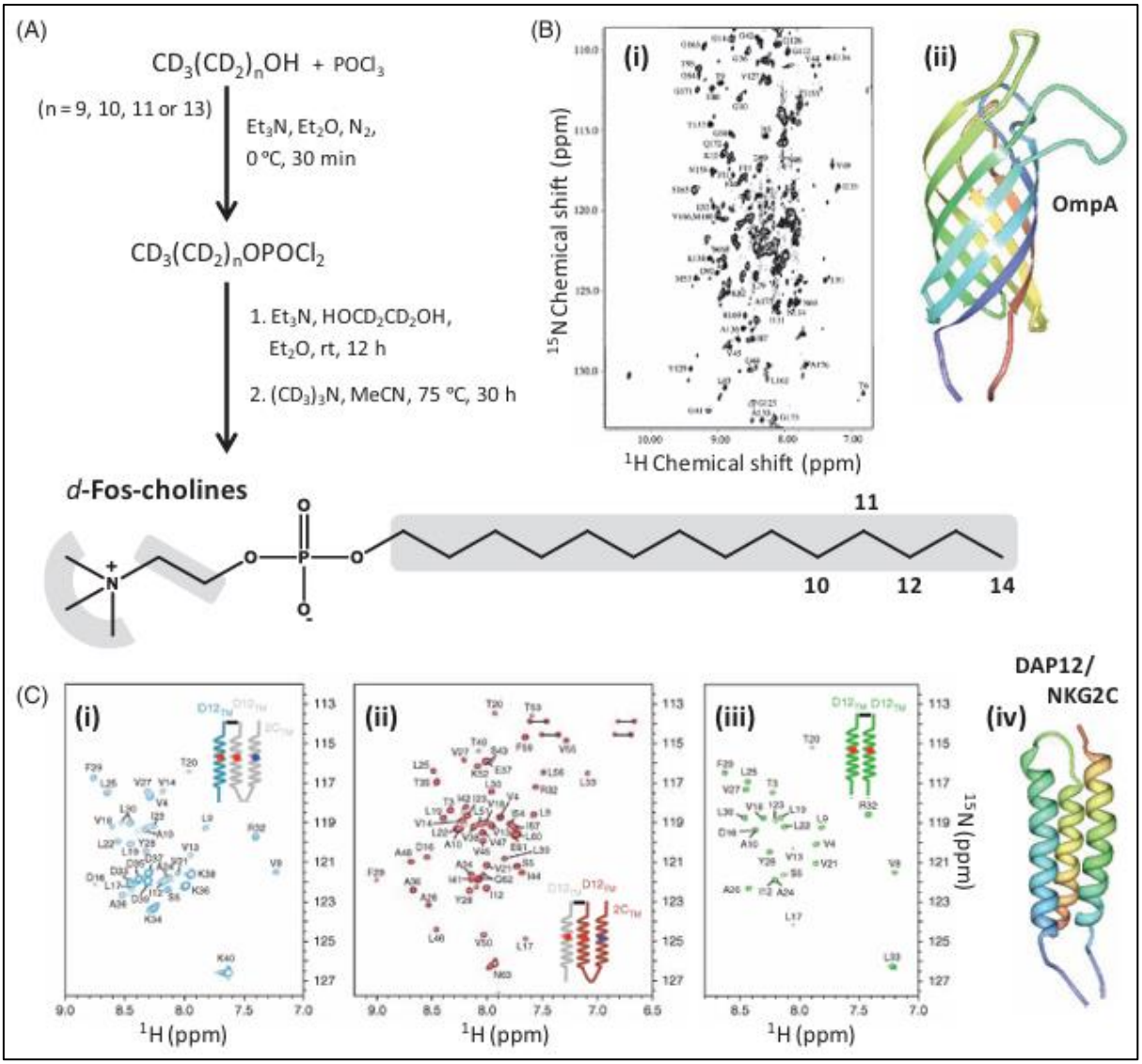

Figure 8: Synthesis of deuterated fos-cholines and use of d_{38}-DPC in solubilizing the bacterial outer membrane protein OmpA and use of d_{42}-fos-choline-14 in solubilizing the human DAP12-NKG2C complex. A. Synthesis of deuterated fos-cholines. The grey areas show the regions of deuteration. B. (i) [^{15}N-^{1}H]TROSY spectrum of OmpA in d_{38}-DPC micelles. (ii) Structure of OmpA with the N-terminus in blue and C-terminus in red, which was drawn using PDB file 1G90 and PDB Protein Workshop 3.9 [188]. C. [^{15}N-^{1}H]HSQC spectra of trimer samples segmentally labeled with ^{15}N-^{2}H on the DAP12-only strand (i) or on the DAP12-NKG2C strand (ii) and of the DAP12 homodimer alone (iii) for samples in 250 mM d_{42}-fos-choline-14 with 25 mM d_{25}-SDS and (iv) structure of the DAP12-NKG2C complex with the N-terminus in blue and C-terminus in red, which was drawn using PDB file 2L35 and PDB Protein Workshop 3.9 [188]. This Figure was reproduced from Hiruma-Shimizu *et al.*, (2015) [12].

NMR structures of α-helical membrane proteins determined in d_{38}-DPC micelles include amyloid precursor protein transmembrane domains [241, 242], phospholamban pentamer phosphorylated at serine 16 [243], HIV-1 envelope glycoprotein gp41 ectodomain [244] and a gp41 envelope membrane proximal region trimer [245] and the 18 kDa mitochondrial translocator protein with a high affinity ligand [246]. The latter protein mediates the uptake of cholesterol and porphyrins into mitochondria and its expression is strongly up regulated in areas of brain injury and in neuroinflammatory conditions. High quality NMR spectra of the protein that enabled structure determination were only achieved for the ligand-bound state. The structure had a tight bundle of five unique transmembrane-spanning a-helices with the ligand positioned towards the cytoplasmic side (Figure 9). Ligand-induced stabilization of the structure led to a proposed molecular mechanism for the stimulation of cholesterol transport into mitochondria [246].

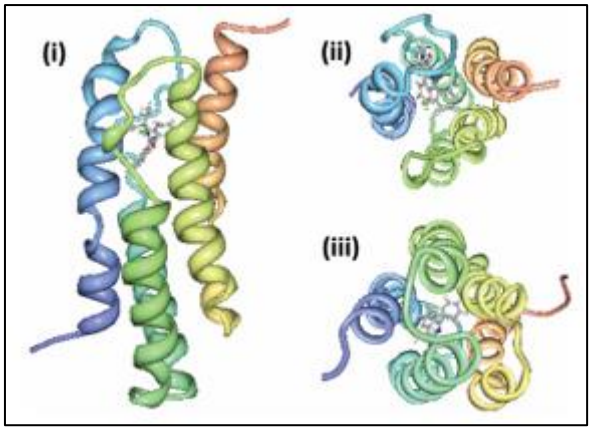

Figure 9: NMR structure of the mitochondrial translocator protein with high affinity ligand determined in d_{38}-DPC micelles. The NMR structure of the mitochondrial translocator protein with high affinity ligand 1-(2-chlorophenyl)-N-methyl-N-(1-methylpropyl)-3-isoquinoline-carboxamide (PK11195) determined in d_{38}-DPC micelles [246] is shown as a side view (i), viewed from the cytoplasm (ii) and viewed from the intermembrane space (iii) with the N-terminus in blue and C-terminus in red, which were drawn using PDB file 2MGY and PDB Protein Workshop 3.9 [188]. This Figure was reproduced from Hiruma-Shimizu *et al.,* (2015) [12].

The NMR structure of the yeast respiratory supercomplex factor Rcf1 (18.5 kDa) was also determined using d_{38}-DPC [247]. Rcf1 forms a dimer in DPC micelles, where each monomer consists of a bundle of five transmembrane α-helices and a short flexible soluble helix (Figure 10).

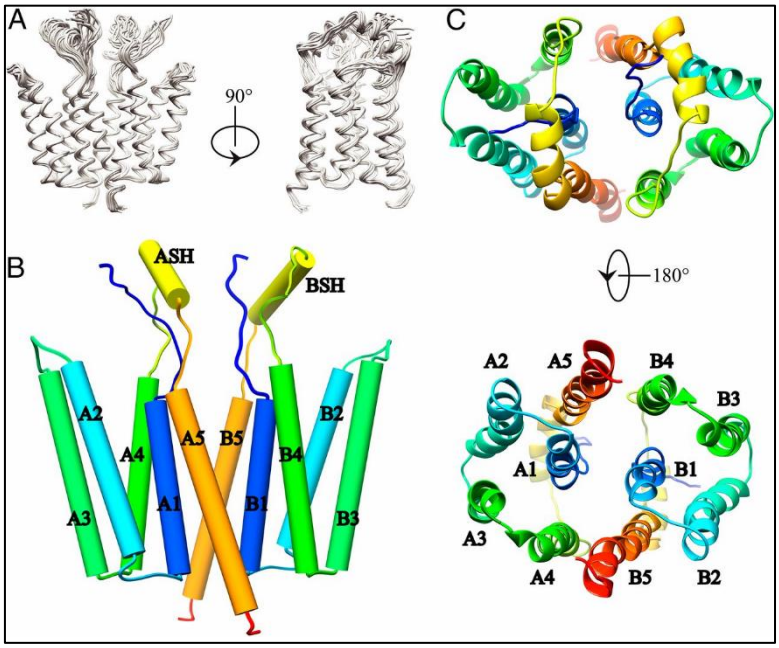

Figure 10: NMR structure of the dimeric Rcf1 in DPC micelles. A. Backbone ribbon trace of the 15 lowest-energy structures determined by solution-state NMR. B. Cylindrical representation of the Rcf1 dimer structure. The five transmembrane α-helices of monomer A (A1-A5), monomer B (B1-B5) and the short flexible soluble helices (ASH, BSH) are shown (see labels). (C) Top view (upper) and bottom view (lower) of the Rcf1 dimer. This figure was reproduced from Zhou *et al.,* (2018) [247].

Deuterated DPC was used in NMR experiments as part of a study on how dynamic proton-dependent motors power type IX secretion and gliding motility in *Flavobacterium johnsoniae* [248]. In this organism secretion and helicoidal motion of the main adhesin SprB are intimately linked and depend on the type IX secretion system (T9SS). These processes use the proton motive force (PMF), which was thought to drive a molecular motor comprised of the cytoplasmic membrane proteins GldL and GldM. NMR was used to investigate whether GldL glutamate residues E49 and E59 undergo protonation and deprotonation cycles. Two-dimensional ^{13}C-HSQC NMR experiments were performed on a ^{15}N/^{13}C Glu-labelled synthetic peptide corresponding to GldL TMH2 (L2, residues Val40 to Val61) in deuterated DPC (form not specified) to determine pKa values. The

carboxylic groups of E49 and E59 had pKa values of 5.54 ± 0.04 and 5.65 ± 0.13, respectively, and further pKa values were measured in the presence of peptides corresponding to GldL TMH1 (L1, residues Lys6 to Thr29) and GldM TMH (M, residues Leu15 to Leu38) (Figure 11). The results demonstrated that GldL and GldM form a cytoplasmic proton channel in which conserved critical glutamate residues are protonated and deprotonated in response to the proton gradient to power both T9SS-dependent secretion and gliding motility [248].

The longer chain d_{42}-Fos-choline-14 was used with d_{25}-SDS in a ratio of 10:1 to solubilize the human DAP12-NKG2C immunoreceptor complex for determination of its NMR structure [151]. The transmembrane domain of the DAP12 signalling molecule has two identical α-helices and the transmembrane domain of the natural killer cell activating receptor NKG2C has one α-helix that packs in an antiparallel orientation along the surface of the DAP12 dimer (Figure 8C).

The structures described here illustrated how DPC and other fos-cholines used to be the most used membrane mimetic for determination of membrane protein structures by solution-state NMR up to around the year 2015. Since then, the realization that alkyl phosphocholine detergents often have destabilizing and denaturing effects on integral membrane proteins has meant that they are not so popular and there has been a move to using milder detergents, such as DDM, where possible.

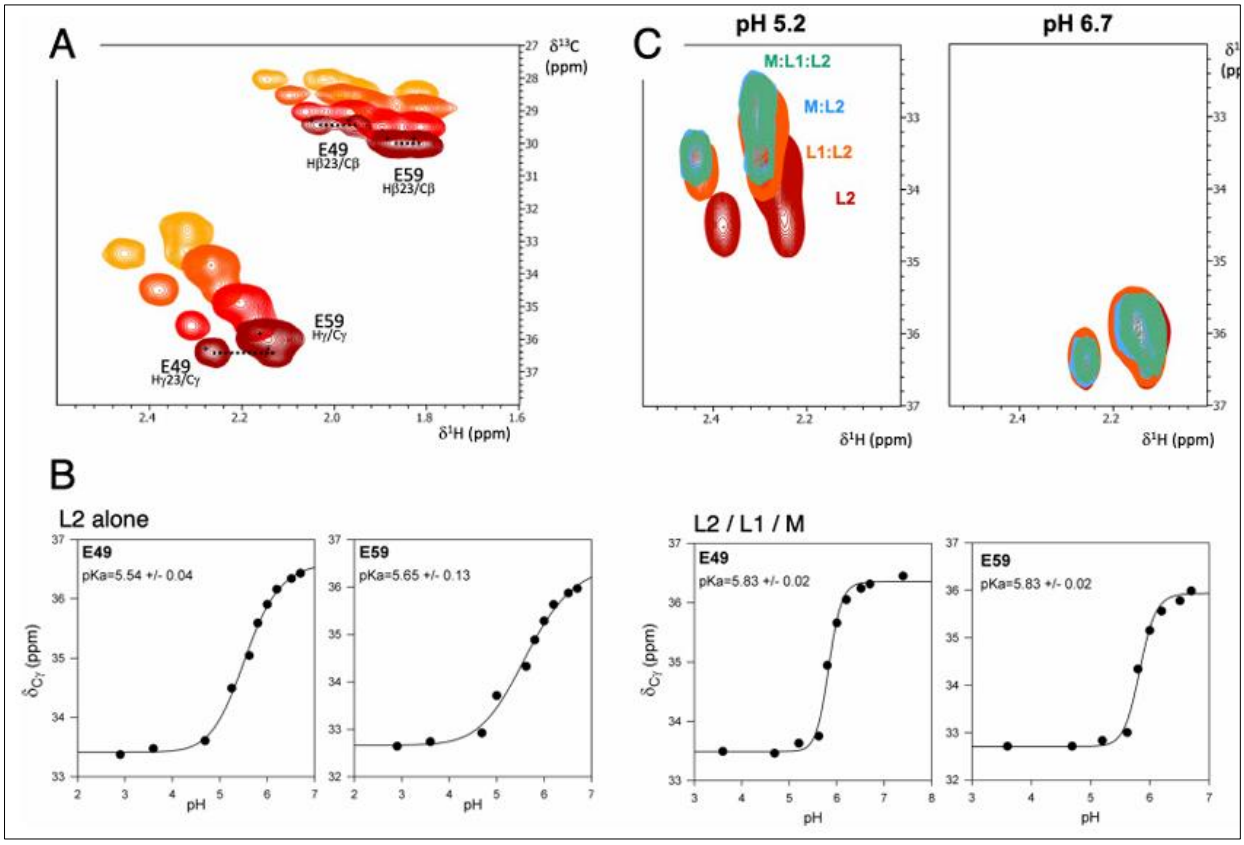

Figure 11: GldL glutamate residues protonation probed by NMR. pKa determination of ^{13}C-Glu free and complexed L2-peptide. A. 2D ^{13}C-HSQC spectra of 1 mM L2 peptide (^{13}C-Glu labeled) in 150 mM deuterated DPC in 50 mM phosphate buffers at different pH (pH 2.9 (yellow), 5.0 (orange), 5.8 (red), 6.7 (brown)). B. The pH dependent chemical shift variations of C_γ carbons of E49 and E59 of the L2 peptide free or complexed with L1 and M in a 1:1:1 molar ratio, were measured, fitted, and apparent pKa values were calculated using the Henderson–Hasselbach equation. C. 2D ^{13}C-HSQC spectra of 1 mM L2 peptide (^{13}C-Glu labeled) in 150 mM deuterated DPC in 50 mM phosphate buffer at pH 5.2 (left panel) and pH 6.7 (right panel), in the absence (brown) and presence at molar ratio 1:1 of GldL-TMH1 peptide (L1, orange), GldM-TMH peptide (M, blue), and both L1 and M peptides (green). This figure was reproduced from Vincent *et al.,* (2022) [248].

4. GUIDELINES FOR DETERGENT SELECTION

To consolidate some guidelines in selecting a suitable detergent for solution-state NMR structural studies of membrane proteins, we can first consider the physical properties of detergent molecules and their effects on micelle formation, protein structure and function, and quality of NMR spectra [12]. These are summarized in Figure 12. Detergent molecules that have

a charged head group, smaller size of head group and shorter length of alkyl chain tend to have lower aggregation numbers and produce smaller micelles and protein-detergent micelle complexes with shorter correlation times. These harsher conditions using detergents such as SDS and its shorter chain versions often produce the best quality NMR spectra, especially for peptides and smaller membrane proteins. On the other hand, these denaturing conditions that produce micelles with a high curvature are not necessarily suitable for retaining the native structural form and activity of the protein. Detergent molecules that have a neutral head group, larger head group and longer alkyl chain tend to have higher aggregation numbers and produce larger micelles and protein-detergent micelle complexes with longer correlation times. These milder conditions using detergents such as DDM and other long chain alkyl glycosides produce micelles with lower curvature and usually retain the native structural form and activity of the protein to a better extent but produce poorer NMR spectra. There are therefore competing tensions in selecting the most suitable detergent for structural studies of membrane proteins using solution-state NMR, SANS and other experimental techniques. The solubility and CMC values of detergent molecules, which are affected by the properties given in Figure 12, also must be considered during sample preparation. For example, the high CMC value of 20–25 mM for β-OG (Table 1) means that a relatively high concentration must be used compared with other detergents. A sample that is stable to days or weeks of NMR data acquisition time at elevated temperatures (typically ≥20 °C) is also required based on current technical capabilities.

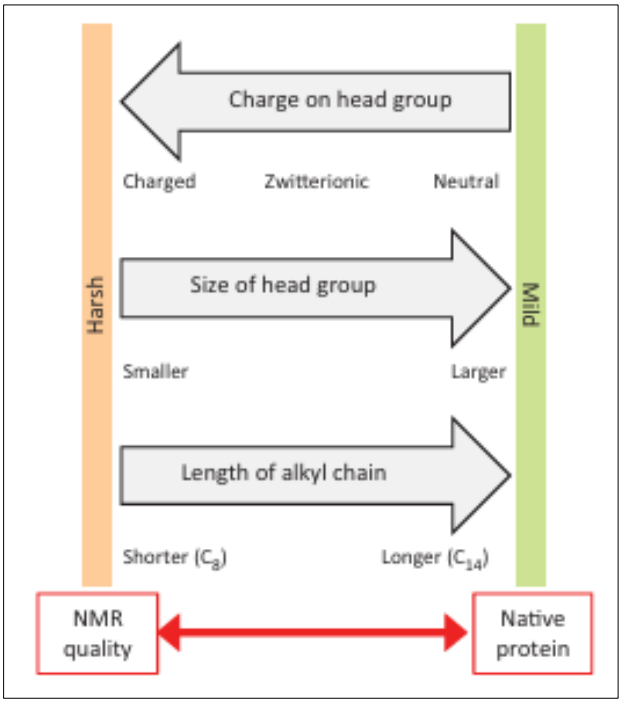

Figure 12: Tensions in selecting a detergent for solution-state NMR structural studies with a membrane protein. This diagram illustrates how the charge on the head group, size of the head group and length of the alkyl group in detergent molecules dictate the properties of detergents and micelle complex formation that provide opposing tensions with regards to achieving good quality NMR spectra and retaining native protein structure and activity. This Figure was reproduced from Hiruma-Shimizu *et al.*, (2015) [12].

We can also look at which detergents have been most successful in producing structures of membrane proteins by solution-state NMR [12]. As mentioned already, by far the most prolific is DPC, which is intermediate on the scale of detergent properties considered in Figure 12 and has solubility and CMC values that are experimentally favourable (Table 1). A detergent that has proved successful for solubilising a certain membrane protein in NMR structural studies may be assumed to be suitable for a different protein of the same type. β-barrel membrane proteins tend to accommodate a relatively wide range of detergents including those with harsher properties that favour better quality NMR spectra, for example LDAO with human VDAC-1 (Figure 3). Large α-helical proteins, such as secondary transporters, are generally restricted to the mildest detergents such as DDM, hence the significant challenges in performing structural studies with these proteins using solution-state NMR. Such proteins likely require some of the native membrane lipids to be carried over into the detergent micelles for retaining their structural and functional integrity, which is facilitated by the milder detergents. Use of a deuterated detergent is generally beneficial and, in some cases, essential for solution-state NMR structural studies of membrane proteins, especially with larger proteins, and it is

© 2025 | Published by Scholars Middle East Publishers, Dubai, United Arab Emirates

important for contrast mapping in SANS experiments [12]. These are only guidelines and not strict rules, but they may be useful in conserving time and materials in the selection of a suitable detergent for structural studies of membrane proteins using solution-state NMR, SANS and other techniques. Experimental investigations still must be performed with each individual protein to identify suitable detergent or other membrane mimetic conditions. There have been some rigorous assessments of how different membrane mimetic environments, including detergents, affect the transmembrane domain structures of α-helical membrane proteins [27, 51, 249]. More work in this area will help in selecting suitable detergents and other membrane mimetics for structural studies of membrane proteins and for achieving native-like structures. With the continued development of NMR techniques for high molecular weight biomolecules and the increasing availability of ultra-field NMR magnets [250], there will likely be a migration to the more common use of milder detergents in solution-state NMR studies of membrane proteins.

5. CONCLUSIONS

This updated and expanded review has emphasized the crucial roles that detergents have in the extraction, purification and stabilization of integral membrane proteins and in experimental studies of their structure and function in solution, especially using solution-state NMR spectroscopy and SANS. It has also highlighted the important role of deuterated detergents in these studies, even though deuterated detergents are relatively expensive and not always commercially available due to challenges associated with their chemical synthesis. Deuterated detergents provide better resolution and sensitivity in NMR spectra, access to overlapped areas of the protein spectrum and simplify the use of more advanced pulse sequences. Proton-detected NMR experiments usually require a deuterated detergent whilst heteronuclear experiments on larger proteins with $^{13}C/^{15}N$ labelling usually benefit from a deuterated detergent. Methyl TROSY based experiments that are required for structure determination of larger membrane proteins also benefit from a deuterated detergent, which is likely to be essential for the most complex proteins. Deuterated detergents are also essential in some SANS studies on membrane proteins, where they can be matched-out to make the detergent “invisible”, which simplifies data analysis. Deuterated detergents will continue to play important roles in structural and functional studies of membrane proteins along with deuterated forms of other membrane mimetics including organic solvents, lipids, bicelles, nanodiscs, styrene maleic acid polymers (SMALPs), fluorinated surfactants and amphipols. Developments in the synthesis and production of deuterated forms of membrane mimetics will continue to evolve and expand along with the world of membrane protein structure, mechanism, ligand interactions and dynamics.

Conflicts of Interest: The authors declare no conflicts of interest.

REFERENCES

1. le Maire, M., Champeil, P., & Moller, J. V. (2000). Interaction of membrane proteins and lipids with solubilizing detergents. Biochim Biophys Acta, 1508(1-2), 86-111.
2. Damberg, P., Jarvet, J., & Gräslund, A. (2001). Micellar systems as solvents in peptide and protein structure determination. Methods Enzymol, 339, 271-285.
3. Garavito, R. M., & Ferguson-Miller, S. (2001). Detergents as tools in membrane biochemistry. J Biol Chem, 276(35), 32403-32406.
4. Seddon, A. M., Curnow, P., & Booth, P. J. (2004). Membrane proteins, lipids and detergents: Not just a soap opera. Biochim Biophys Acta, 1666(1-2), 105-117.
5. Privé, G. G. (2007). Detergents for the stabilization and crystallization of membrane proteins. Methods, 41(4), 388-397.
6. Kim, H. J., Howell, S. C., Van Horn, W. D., Jeon, Y. H, & Sanders, C. R. (2009). Recent advances in the application of solution NMR spectroscopy to multi-span integral membrane proteins. Prog Nucl Magn Reson Spectrosc, 55(4), 335-360.
7. Arnold, T., & Linke, D. (2008). The use of detergents to purify membrane proteins. Curr Protoc Protein Sci, Chapter 4: Unit 4.8.1-4.8.30.
8. Lin, S. H., & Guidotti, G. (2009). Purification of membrane proteins. Methods Enzymol, 463, 619-629.
9. Linke, D. (2009). Detergents: An overview. Methods Enzymol, 463, 603-617.
10. Sonoda, Y., Newstead, S., Hu, N. J., Alguel, Y., Nji, E., Beis, K., Yashiro, S., Lee, C., Leung, J., Cameron, A. D., Byrne, B., Iwata, S., & Drew, D. (2011). Benchmarking membrane protein detergent stability for improving throughput of high-resolution X-ray structures. Structure, 19(1), 17-25.
11. Arachea, B. T., Sun, Z., Potente, N., Malik, R., Isailovic, D., & Viola, R. E. (2012). Detergent selection for enhanced extraction of membrane proteins. Protein Expr Purif, 86(1), 12-20.
12. Hiruma-Shimizu, K., Shimizu, H., Thompson, G. S., Kalverda, A. P., & Patching, S. G. (2015). Deuterated detergents for structural and functional studies of membrane proteins: Properties, chemical synthesis and applications. Mol Membr Biol, 32(5-8), 139-155.
13. Breibeck, J., & Rompel, A. (2019). Successful amphiphiles as the key to crystallization of membrane proteins: Bridging theory and practice. Biochim Biophys Acta Gen Subj, 1863(2), 437-455.
14. Kermani, A. A. (2021). A guide to membrane protein X-ray crystallography. FEBS J, 288(20), 5788-5804.

15. Li, S. (2022). Detergents and alternatives in cryo-EM studies of membrane proteins. Acta Biochim Biophys Sin (Shanghai), 54(8), 1049-1056.
16. Behnke, J. S., & Urner, L. H. (2023). Emergence of mass spectrometry detergents for membrane proteomics. Anal Bioanal Chem, (18), 3897-3909.
17. Brough, Z., Zhao, Z., & Duong van Hoa, F. (2024). From bottom-up to cell surface proteomics: detergents or no detergents, that is the question. Biochem Soc Trans, 52(3), 1253-1263.
18. Woubshete, M., Cioccolo, S., & Byrne, B. (2024). Advances in membrane mimetic systems for manipulation and analysis of membrane proteins: Detergents, polymers, lipids and scaffolds. Chempluschem, 89(6), e202300678.
19. Cheng, D., Guo, Y., Lyu, J., Liu, Y., Xu, W., Zheng, W., Wang, Y., & Qiao, P. (2025). Advances and challenges in preparing membrane proteins for native mass spectrometry. Biotechnol Adv, 78, 108483.
20. Zhou, Z., Chen, Z., Li, Y., Mao, X., Chen, J., Zhou, X., & Zhang, B. (2025). Advances in solubilization and stabilization techniques for structural and functional studies of membrane proteins. PeerJ, 13, e19211.
21. Bayburt, T. H., & Sligar, S. G. (2010). Membrane protein assembly into nanodiscs. FEBS Lett, 584(9), 1721-1727.
22. Popot, J. L. (2020). Amphipols, nanodiscs, and fluorinated surfactants: Three nonconventional approaches to studying membrane proteins in aqueous solutions. Annu Rev Biochem, 79, 737-775.
23. Warschawski, D. E, Arnold, A. A, Beaugrand, M., Gravel, A., Chartrand, É., & Marcotte, I. (2011). Choosing membrane mimetics for NMR structural studies of transmembrane proteins. Biochim Biophys Acta, 1808(8), 1957-1974.
24. Dürr, U. H., Gildenberg, M., & Ramamoorthy, A. (2012). The magic of bicelles lights up membrane protein structure. Chem Rev, 112(11), 6054-6074.
25. Dürr, U. H., Soong, R., & Ramamoorthy, A. (2013). When detergent meets bilayer:Bbirth and coming of age of lipid bicelles. Prog Nucl Magn Reson Spectrosc, 69, 1-22.
26. Inagaki, S., Ghirlando, R., & Grisshammer, R. (2013). Biophysical characterization of membrane proteins in nanodiscs. Methods, 59(3), 287-300.
27. Zhou, H. X, & Cross, T. A. (2013). Influences of membrane mimetic environments on membrane protein structures. Annu Rev Biophys, 42, 361-392.
28. Zoonens, M., & Popot, J. L. (2014). Amphipols for each season. J Membr Biol, 247(9-10), 759-796.
29. Marty, M. T., Hoi, K. K., & Robinson, C. V. (2016). Interfacing membrane mimetics with mass spectrometry. Acc Chem Res, 49(11), 2459-2467.
30. Frey, L., Lakomek, N. A., Riek, R., & Bibow, S. (2017). Micelles, bicelles, and nanodiscs: Comparing the impact of membrane mimetics on membrane protein backbone dynamics. Angew Chem Int Ed Engl, 56(1), 380-383.
31. Esmaili, M., & Overduin, M. (2018). Membrane biology visualized in nanometer-sized discs formed by styrene maleic acid polymers. Biochim Biophys Acta Biomembr, 1860(2), 257-263.
32. Stroud, Z., Hall, S. C. L., & Dafforn, T. R. (2018). Purification of membrane proteins free from conventional detergents: SMA, new polymers, new opportunities and new insights. Methods, 147, 106-117.
33. Klöpfer, K., & Hagn, F. (2019). Beyond detergent micelles: The advantages and applications of non-micellar and lipid-based membrane mimetics for solution-state NMR. Prog Nucl Magn Reson Spectrosc, 114-115, 271-283.
34. Thoma, J., & Burmann, B. M. (2020). Fake it 'till you make it-the pursuit of suitable membrane mimetics for membrane protein biophysics. Int J Mol Sci, 22(1), 50.
35. Wiseman, D. N., Otchere, A., Patel, J. H., Uddin, R., Pollock, N. L., Routledge, S. J., Rothnie, A. J., Slack, C., Poyner, D. R., Bill, R. M., & Goddard, A. D. (2020). Expression and purification of recombinant G protein-coupled receptors: A review. Protein Expr Purif, 167, 105524.
36. Choy, B. C., Cater, R. J., Mancia, F., & Pryor, E. E. Jr. (2021). A 10-year meta-analysis of membrane protein structural biology: Detergents, membrane mimetics, and structure determination techniques. Biochim Biophys Acta Biomembr, 1863(3), 183533.
37. Majeed, S., Ahmad, A. B., Sehar, U., & Georgieva, E. R. (2021). Lipid membrane mimetics in functional and structural studies of integral membrane proteins. Membranes (Basel), 11(9), 685.
38. Sahu, I. D., & Lorigan, G. A. (2023). Role of membrane mimetics on biophysical EPR studies of membrane proteins. Biochim Biophys Acta Biomembr, 1865(4), 184138.
39. Young, J. W. (2023). Recent advances in membrane mimetics for membrane protein research. Biochem Soc Trans, 51(3), 1405-1416.
40. Page, R. C., Moore, J. D., Nguyen, H. B., Sharma, M., Chase, R., Gao, F. P., Mobley, C. K., Sanders, C. R., Ma, L., Sönnichsen, F. D., Lee, S., Howell, S. C., Opella, S. J., & Cross, T. A. (2006). Comprehensive evaluation of solution nuclear magnetic resonance spectroscopy sample preparation for helical integral membrane proteins. J Struct Funct Genomics, 7(1), 51-64.
41. Nietlispach, D., & Gautier, A. (2011). Solution NMR studies of polytopic α-helical membrane proteins. Curr Opin Struct Biol, 21(4), 497-508.
42. Patching, S. G. (2011). NMR structures of polytopic integral membrane proteins. Mol Membr Biol, 28(6), 370-397.
43. Klammt, C., Maslennikov, I., Bayrhuber, M., Eichmann, C., Vajpai, N., Chiu, E. J., Blain, K. Y., Esquivies, L., Kwon, J. H., Balana, B., Pieper, U.,

Sali, A., Slesinger, P. A., Kwiatkowski, W., Riek, R., & Choe, S. (2012). Facile backbone structure determination of human membrane proteins by NMR spectroscopy. Nat Methods, 9(8), 834-839.
44. Arora, A. (2013). Solution NMR spectroscopy for the determination of structures of membrane proteins in a lipid environment. Methods Mol Biol, 974, 389-413.
45. Maslennikov, I., & Choe, S. (2013). Advances in NMR structures of integral membrane proteins. Curr Opin Struct Biol, 23(4), 555-562.
46. Reckel, S., & Hiller, S. (2013). Perspectives of solution NMR spectroscopy for structural and functional studies of integral membrane proteins. Molec Phys, 111(7), 843-849.
47. Patching, S. G. (2016). NMR-active nuclei for biological and biomedical applications. J Diagn Imag Ther, 3(1), 7-48.
48. Danmaliki, G. I., & Hwang, P. M. (2020). Solution NMR spectroscopy of membrane proteins. Biochimica et Biophysica Acta (BBA) – Biomembranes, 1862(9), 183356.
49. Raman, P., Cherezov, V., & Caffrey. M. (2006). The membrane protein data bank. Cell Mol Life Sci, 63(1), 36-51.
50. Oliver, R. C., Lipfert, J., Fox, D. A., Lo, R. H., Doniach, S., & Columbus, L. (2013). Dependence of micelle size and shape on detergent alkyl chain length and head group. PLoS One, 8(5), e62488.
51. Chipot, C., Dehez, F., Schnell, J. R., Zitzmann, N., Pebay-Peyroula, E., Catoire, L. J., Miroux, B., Kunji, E. R. S., Veglia, G., Cross, T. A., & Schanda, P. (2018). Perturbations of native membrane protein structure in alkyl phosphocholine detergents: A critical assessment of NMR and biophysical studies. Chem Rev, 118(7), 3559-3607.
52. Brown, L. R. (1979). Use of fully deuterated micelles for conformational studies of membrane proteins by high resolution ^{1}H nuclear magnetic resonance. Biochim Biophys Acta, 557(1), 135-148.
53. Brown, L. R., & Wűthrich, K. (1981). Melittin bound to dodecylphosphocholine micelles. H-NMR assignments and global conformational features. Biochim Biophys Acta, 647(1), 95-111.
54. Arora, A., & Tamm, L. K. (2001). Biophysical approaches to membrane protein structure determination. Curr Opin Struct Biol, 11(5), 540-547.
55. Hiller, S., & Wagner, G. (2009). The role of solution NMR in the structure determinations of VDAC-1 and other membrane proteins. Curr Opin Struct Biol, 19(4), 396-401.
56. Heller, W. T. (2010). Small-angle neutron scattering and contrast variation: a powerful combination for studying biological structures. Acta Crystallogr D Biol Crystallogr, 66(Pt 11), 1213-1217.
57. Breyton, C., Gabel, F., Lethier, M., Flayhan, A., Durand, G., Jault, J. M., Juillan Binard, C., Imbert, L., Moulin, M., Ravaud, S., Härtlein, M., & Ebel, C. (2013). Small angle neutron scattering for the study of solubilised membrane proteins. Eur Phys J E Soft Matter, 36(7), 71.
58. Gabel, F. (2017). Applications of SANS to study membrane protein systems. Adv Exp Med Biol, 1009, 201-214.
59. Koutsioubas, A. (2017). Low-resolution structure of detergent-solubilized membrane proteins from small-angle scattering data. Biophys J, 113(11), 2373-2382.
60. Krueger, S. (2017). Designing and performing biological solution small-angle neutron scattering contrast variation experiments on multi-component assemblies. Adv Exp Med Biol, 1009, 65-85.
61. Mahieu, E., & Gabel, F. (2018). Biological small-angle neutron scattering: recent results and development. Acta Crystallogr D Struct Biol, 74(Pt 8), 715-726.
62. Oliver, R. C., Naing, S. H., Weiss, K. L., Pingali, S. V., Lieberman, R. L., & Urban, V. S. (2018). Contrast-matching detergent in small-angle neutron scattering experiments for membrane protein structural analysis and ab initio modeling. J Vis Exp, 140, 57901.
63. Ebel, C., Breyton, C., & Martel, A. (2020). Examining membrane proteins by neutron scattering. Methods Mol Biol, 2168, 147-175.
64. Morrison, K. A., Doekhie, A., Neville, G. M., Price, G. J., Whitley, P., Doutch, J., & Edler, K. J. (2021). Ab initio reconstruction of small angle scattering data for membrane proteins in copolymer nanodiscs. BBA Adv, 2, 100033.
65. Josts, I., Kehlenbeck, D. M., Nitsche, J., & Tidow, H. (2022). Studying integral membrane protein by SANS using stealth reconstitution systems. Methods Enzymol, 677, 417-432.
66. Adhikari, L., Mishra, H., Semalty, M., & Semalty, A. (2023). Small angle neutron scattering in drug discovery research: A novel tool for advanced study of structures of biological macromolecules. Curr Drug Discov Technol, 20(5), e150523216942.
67. Dunne, O., Weidenhaupt, M., Callow, P., Martel, A., Moulin, M., Perkins, S. J., Haertlein, M., & Forsyth, V. T. (2017). Matchout deuterium labelling of proteins for small-angle neutron scattering studies using prokaryotic and eukaryotic expression systems and high cell-density cultures. Eur Biophys J, 46(5), 425-432.
68. Yogo, R., Yanaka, S., Yagi, H., Martel, A., Porcar, L., Ueki, Y., Inoue, R., Sato, N., Sugiyama, M., & Kato, K. (2017). Characterization of conformational deformation-coupled interaction between immunoglobulin G1 Fc glycoprotein and a low-affinity Fcγ receptor by deuteration-assisted small-angle neutron scattering. Biochem Biophys Rep, 12, 1-4.
69. Wu, Y., Weiss, K. L., & Lieberman, R. L. (2021). Preparation of a deuterated membrane protein for small-angle neutron scattering. Methods Mol Biol, 2302, 219-235.

70. Duff, A. P., Cagnes, M., Darwish, T. A., Krause-Heuer, A. M., Moir, M., Recsei, C., Rekas, A., Russell, R. A., Wilde, K. L., & Yepuri, N. R. (2022). Deuteration for biological SANS: Case studies, success and challenges in chemistry and biology. Methods Enzymol, 677, 85-126.
71. Heller, W. T. (2022). Small-angle neutron scattering for studying lipid bilayer membranes. Biomolecules, 12(11), 1591.
72. Chen, S. H., Weiss, K. L., Stanley, C., & Bhowmik, D. (2023). Structural characterization of an intrinsically disordered protein complex using integrated small-angle neutron scattering and computing. Protein Sci, 32(10), e4772.
73. Golub, M., & Pieper, J. (2023). Recent progress in solution structure studies of photosynthetic proteins using small-angle scattering methods. Molecules, 28(21), 7414.
74. Munsayac, A., Leite, W. C., Hopkins, J. B., Hall, I., O'Neill, H. M., & Keane, S. C. (2025). Selective deuteration of an RNA:RNA complex for structural analysis using small-angle scattering. Structure, 33(4), 728-739.
75. Andreeva, B. M. (2001). Separation of hydrogen isotopes in H_2O-H_2S system. Separat Sci Technol, 36(8-9), 1949-1989.
76. Urey, H. C., Brickwedde, F. G., & Murphy, G. M. (1932). A hydrogen isotope of mass 2 and its concentration. Phys Rev, 39, 164.
77. Washburn, E. W., & Urey, H. C. (1932). Concentration of the H isotope of hydrogen by the fractional electrolysis of water. Proc Natl Acad Sci USA, 18(7), 496-498.
78. Katz, J. J. (1965). Chemical and biological studies with deuterium. Pennsylvania: Pennsylvania State University, University Park, 1-100.
79. Thomas, A. F. (1971). Deuterium labeling in organic chemistry. New York: Appleton-Century.
80. Wiberg, K. B. (1955). The deuterium isotope effect. Chem Rev, 55(4), 713-743.
81. Westheimer, F. H. (1961). The magnitude of the primary kinetic isotope effect for compounds of hydrogen and deuterium. Chem Rev, 61, 265-273.
82. Bigeleisen, J., & Goeppert-Mayer, M. (1947). Calculation of equilibrium constants for isotopic exchange reaction. J Phys Chem, 15(5), 261-267.
83. Saunders, W. H. Jr, & Edison, D. H. (1960). Mechanisms of elimination reactions. IV. Deuterium isotope effects in E2 reactions of some 2-phenylethyl derivatives. J Am Chem Soc, 82(1), 138-142.
84. Pascal, R. A., Baum, M. W., Wagner, C. K., Rodgers, L. R., & Huang, D. S. (1986). Measurement of deuterium kinetic isotope effects in organic and biochemical reactions by natural abundance deuterium NMR spectroscopy. J Am Chem Soc, 108(21), 6477-6482.
85. Yu, P. H., Durden, D. A., Davis, B. A., & Boulton, A. A. (1987). Deuterium isotope effect in gamma-aminobutyric acid transamination: determination of rate-limiting step. J Neurochem, 48(2), 440-446.
86. Krumbiegel, P. (2011). Large deuterium isotope effects and their use: A historical review. Isotopes Environ Health Stud, 47(1), 1-17.
87. Pedras, M. S., Minic, Z., & Sarma-Mamillapalle, V. K. (2011). Brassinin oxidase mediated transformation of the phytoalexin brassinin: Structure of the elusive co-product, deuterium isotope effect and stereoselectivity. Bioorg Med Chem, 19(4), 1390-1399.
88. Isaacs, N. S. (1987). Physical organic chemistry. New York: Longman.
89. Wade, D. (1999). Deuterium isotope effects on noncovalent interactions between molecules. Chem Biol Interact, 117(3), 191-217.
90. Hoffman, J. M., Habecker, C. N., Pietruszkiewicz, A. M., Bolhofer, W. A., Cragoe Jr, E. J., Torchiana, M. L., & Hirschmann, R. (1983). A deuterium isotope effect on the inhibition of gastric secretion by N,N-dimethyl-N0-[2-(diisopropylamino)ethyl]-N0-(4,6-dimethyl-2-pyridyl)urea. Synthesis of metabolites. J Med Chem, 26(11), 1650-1653.
91. White, R. D., Gandolfi, A. J., Bowden, G. T., & Sipes, I. G. (1983). Deuterium isotope effect on the metabolism and toxicity of 1,2-dibromoethane. Toxicol Appl Pharmacol, 69(2), 170-178.
92. Baldwin, J. E., Gallagher, S. S., Leber, P. A., Raghavan, A. S., & Shukla, R. (2004). Deuterium kinetic isotope effects and mechanism of the thermal isomerization of bicyclo[4.2.0]oct-7-ene to 1,3-cyclooctadiene. J Org Chem, 69(21), 7212-7219.
93. Cleland, W. W. (2005). The use of isotope effects to determine enzyme mechanisms. Arch Biochem Biophys, 433(1), 2-12.
94. He, X., Morris, J. J., Noll, B. C., Brown, S. N., & Henderson, K. W. (2006). Kinetics and mechanism of ketone enolization mediated by magnesium bis(hexamethyldisilazide). J Am Chem Soc, 128(41), 13599-13610.
95. Shao, L., & Hewitt, M. C. (2010). The kinetic isotope effect in the search for deuterated drugs. Drug News Perspect, 23(6), 398-404.
96. Sharma, R., Strelevitz, T. J., Gao, H., Clark, A. J., Schildknegt, K., Obach, R. S., Ripp, S. L., Spracklin, D. K., Tremaine, L. M., & Vaz, A. D. (2012). Deuterium isotope effects on drug pharmacokinetics. I. System-dependent effects of specific deuteration with aldehyde oxidase cleared drugs. Drug Metab Dispos, 40(3), 625-634.
97. Simmons, E. M., & Hartwig, J. F. (2012). On the interpretation of deuterium kinetic isotope effects in C-H bond functionalizations by transition-metal complexes. Angew Chem Int, 51(13), 3066-3072.
98. Manley, P. W., Blasco, F., Mestan, J., & Aichholz, R. (2013). The kinetic deuterium isotope effect as applied to metabolic deactivation of imatinib to the des-methyl metabolite, CGP74588. Bioorg Med Chem, 21(11), 3231-3239.

99. Guengerich, F. P. (2013). Kinetic deuterium isotope effects in cytochrome P450 oxidation reactions. J Labelled Comp Radiopharm, 56(9-10), 428-431.
100. Timmins, G. S. (2014). Deuterated drugs: Where are we now? Expert Opin Ther Pat, 24(10), 1067-1075.
101. Murad, S., Chen, R. H., & Kishimoto, Y. (1977). alpha-Hydroxylation of fatty acids in brain. Substrate specificity and deuterium isotope effect. J Biol Chem, 252(15), 5206-5210.
102. Yang, C. S, & Ishizaki, H. (1992). Deuterium isotope effect on the metabolism of N-nitrosodimethylamine and related compounds by cytochrome P4502E1. Xenobiotica, 22(9-10), 1165-1173.
103. Hochuli, M., Szyperski, T., & Wűthrich, K. (2000). Deuterium isotope effects on the central carbon metabolism of *Escherichia coli* cells grown on a D_2O-containing minimal medium. J Biomol NMR, 17(1), 33-42.
104. Mittermaier, A., & Kay, L. E. (2002). Effect of deuteration on some structural parameters of methyl groups in proteins as evaluated by residual dipolar couplings. J Biomol NMR, 23(1), 35-45.
105. Fisher, S. J., & Helliwell, J. R. (2008). An investigation into structural changes due to deuteration. Acta Crystallogr A, 64(Pt 3), 359-367.
106. de Ghellinck, A., Schaller, H., Laux, V., Haertlein, M., Sferrazza, M., Maréchal, E., Wacklin, H., Jouhet, J., & Fragneto, G. (2014). Production and analysis of perdeuterated lipids from *Pichia pastoris* cells. PLoS One, 9(4), e92999.
107. Kelly, S. M., & Price, N. C. (2000). The use of circular dichroism in the investigation of protein structure and function. Curr Protein Pept Sci, 1(4), 349-384.
108. Miles, A. J., & Wallace, B. A. (2006). Synchrotron radiation circular dichroism spectroscopy of proteins and applications in structural and functional genomics. Chem Soc Rev, 35(1), 39-51.
109. Patching, S. G., Edara, S., Ma, P., Nakayama, J., Hussain, R., Siligardi, G., & Phillips-Jones, M. K. (2012). Interactions of the intact FsrC membrane histidine kinase with its pheromone ligand GBAP revealed through synchrotron radiation circular dichroism. Biochim Biophys Acta, 1818(7), 1595-1602.
110. Bettaney, K. E., Sukumar, P., Hussain, R., Siligardi, G., Henderson, P. J., & Patching, S. G. (2013). A systematic approach to the amplified expression, functional characterization and purification of inositol transporters from *Bacillus subtilis*. Mol Membr Biol, 30(1), 3-14.
111. Matsuo, K., & Gekko, K. (2019). Circular-dichroism and synchrotron-radiation circular-dichroism spectroscopy as tools to monitor protein structure in a lipid environment. Methods Mol Biol, 2003, 253-279.
112. Siligardi, G., Hussain, R., Patching, S. G., & Phillips-Jones, M. K. (2014). Ligand and drug-binding studies of membrane proteins revealed through circular dichroism spectroscopy. Biochim Biophys Acta, 1838(1 Pt A), 34-42.
113. Ahmad, I., Ma, P., Nawaz, N., Sharples, D. J., Henderson, P. J. F., & Patching, S. G. (2020). Cloning, amplified expression, functional characterisation and purification of *Vibrio parahaemolyticus* NCS1 cytosine transporter VPA1242. Chapter 8. In: Patching SG (Ed) A Closer Look at Membrane Proteins. Independent Publishing Network, pp. 241-267. ISBN: 978-1-83853-535-3.
114. Ahmad, I., Hassan, K. A., Henderson, P. J. F., & Patching, S. G. (2022). Cloning, amplified expression, functional characterisation and purification of a *Pseudomonas putida* NCS1 family transport protein. Int J Adv Multidiscip Res, 9(12), 127-156.
115. Patching, S. G. (2022). Spermidine binding to the *Acetinobacter baumannii* efflux protein AceI observed by near-UV synchrotron radiation circular dichroism spectroscopy. Radiation, 2(2), 228-233.
116. Ali, M., Ali, R., Khan, I. A., Ahmad, I., Nawaz, N., & Patching, S. G. (2025). The *Escherichia coli* zinc exporter ZitB of the Cation Diffusion Facilitator (CDF) protein family: Properties, cloning, amplified expression, purification. Sch Int J Biochem, 8(2), 50-65.
117. Kalverda, A. P., Gowdy, J., Thompson, G. S., Homans, S. W., Henderson, P. J., & Patching, S. G. (2014). TROSY NMR with a 52 kDa sugar transport protein and the binding of a small-molecule inhibitor. Mol Membr Biol, 31(4), 131-140.
118. Alexandrov, A. I., Mileni, M., Chien, E. Y., Hanson, M. A., & Stevens, R. C. (2008). Microscale fluorescent thermal stability assay for membrane proteins. Structure, 16(3), 351-359.
119. Kotov, V., Bartels, K., Veith, K., Josts, I., Subhramanyam, U. K. T., Günther, C., Labahn, J., Marlovits, T. C., Moraes, I., Tidow, H., Löw, C., & Garcia-Alai, M. M. (2019). High-throughput stability screening for detergent-solubilized membrane proteins. Sci Rep, 9(1), 10379.
120. Goñi, F. M., & Alonso, A. (2000). Spectroscopic techniques in the study of membrane solubilization, reconstitution and permeabilization by detergents. Biochim Biophys Acta, 1508(1-2), 51-68.
121. Postis, V. L., Deacon, S. E., Roach, P. C., Wright, G. S., Xia, X., Ingram, J. C., Hadden, J. M., Henderson, P. J., Phillips, S. E., McPherson., M. J., & Baldwin, S. A. (2008). A high-throughput assay of membrane protein stability. Mol Membr Biol, 25(8), 617-624.
122. Slotboom, D. J., Duurkens, R. H., Olieman, K., & Erkens, G. B. (2008). Static light scattering to characterize membrane proteins in detergent solution. Methods, 46(2), 73-82.
123. Neale, C., Ghanei, H., Holyoake, J., Bishop, R. E., Privé, G. G., & Pomès, R. (2013). Detergent-mediated protein aggregation. Chem Phys Lipids, 169, 72-84.

© 2025 | Published by Scholars Middle East Publishers, Dubai, United Arab Emirates

124. Meyer, A., Dierks, K., Hussein, R., Brillet, K., Brognaro, H., & Betzel, C. (2015). Systematic analysis of protein-detergent complexes applying dynamic light scattering to optimize solutions for crystallization trials. Acta Crystallogr F Struct Biol Commun, 71(Pt 1), 75-81.
125. Vergis, J. M., Purdy, M. D., & Wiener, M. C. (2010). A high-throughput differential filtration assay to screen and select detergents for membrane proteins. Anal Biochem, 407(1), 1-11.
126. Maslennikov, I., Kefala, G., Johnson, C., Riek, R., Choe, S., & Kwiatkowski, W. (2007). NMR spectroscopic and analytical ultracentrifuge analysis of membrane protein detergent complexes. BMC Struct Biol, 7, 74.
127. Klammt, C., Schwarz, D., Fendler, K., Haase, W., Dötsch, V., & Bernhard, F. (2005). Evaluation of detergents for the soluble expression of alpha-helical and beta-barrel-type integral membrane - proteins by a preparative scale individual cell-free expression system. FEBS, 272(23), 6024-6038.
128. Yeh, A. P., McMillan, A., & Stowell, M. H. (2006). Rapid and simple protein stability screens: Application to membrane proteins. Acta Crystallogr D Biol Crystallogr, 62(Pt 4), 451-457.
129. Tate, C. G. (2010). Practical considerations of membrane protein instability during purification and crystallisation. Methods Mol Biol, 601, 187-203.
130. Kang, H. J., Lee, C., & Drew, D. (2013). Breaking the barriers in membrane protein crystallography. Int J Biochem Cell Biol, 45(3), 636-644.
131. Stetsenko, A., & Guskov, A. (2017). An overview of the top ten detergents used for membrane protein crystallization. Crystals, 7(7), 197.
132. Gorrec, F., & Bellini, D. (2022). The FUSION protein crystallization screen. J Appl Crystallogr, 55(Pt 2), 310-319.
133. Krueger-Koplin, R. D., Sorgen, P. L., Krueger-Koplin, S. T., Rivera-Torres, I. O., Cahill, S. M., Hicks, D. B., Grinius, L., Krulwich, T. A., & Girvin, M. E. (2004). An evaluation of detergents for NMR structural studies of membrane proteins. J Biomol NMR, 28(1), 43-57.
134. Chen, L., Lai, C., Lai, J., & Tian, C. (2011). Expression, purification, detergent screening and solution NMR backbone assignment of the human potassium channel accessory subunit MiRP1. Protein Expr Purif, 76(2), 205-210.
135. Horst, R., Horwich, A. L., & Wüthrich, K. (2011). Translational diffusion of macromolecular assemblies measured using transverse-relaxation-optimized pulsed field gradient NMR. J Am Chem Soc, 133(41), 16354-16357.
136. Yao, S., Weber, D. K., Separovic, F., & Keizer, D. W. (2014). Measuring translational diffusion coefficients of peptides and proteins by PFG NMR using band-selective RF pulses. Eur Biophys J, 43(6-7), 331-339.
137. Korchuganov, D. S., Gagnidze, I. E., Tkach, E. N., Schulga, A. A., Kirpichnikov, M. P., & Arseniev, A. S. (2004). Determination of protein rotational correlation time from NMR relaxation data at various solvent viscosities. J Biomol NMR, 30(4), 431-442.
138. Lee, D., Hilty, C., Wider, G., & Wüthrich, K. (2006). Effective rotational correlation times of proteins from NMR relaxation interference. J Magn Reson, 178(1), 72-76.
139. Zhang, Q., Horst, R., Geralt, M., Ma, X., Hong, W. X., Finn, M. G., Stevens, R. C., & Wüthrich, K. (2008). Microscale NMR screening of new detergents for membrane protein structural biology. J Am Chem Soc, 130(23), 7357-7363.
140. Stanczak, P., Horst, R., Serrano, P., & Wüthrich, K. (2009). NMR characterization of membrane protein-detergent micelle solutions by use of microcoil equipment. J Am Chem Soc, 131(51), 18450-18456.
141. Horst, R., Stanczak, P., Serrano, P., & Wüthrich, K. (2012). Translational diffusion measurements by microcoil NMR in aqueous solutions of the Fos-10 detergent-solubilized membrane protein OmpX. J Phys Chem B, 116(23), 6775-6780.
142. Stanczak, P., Zhang, Q., Horst, R., Serrano, P., & Wüthrich, K. (2012). Micro-coil NMR to monitor optimization of the reconstitution conditions for the integral membrane protein OmpW in detergent micelles. J Biomol NMR, 54(2), 129-133.
143. Columbus, L., Lipfert, J., Jambunathan, K., Fox, D. A., Sim, A. Y., Doniach, S., & Lesley, S. A. (2009). Mixing and matching detergents for membrane protein NMR structure determination. J Am Chem Soc, 131(21), 7320-7326.
144. O'Malley, M. A., Helgeson, M. E., Wagner, N. J., & Robinson, A. S. (2011). Toward rational design of protein detergent complexes: Determinants of mixed micelles that are critical for the in vitro stabilization of a G-protein coupled receptor. Biophys J, 101(8), 1938-1948.
145. Nadeau, V. G., Rath, A., & Deber, C. M. (2012). Sequence hydropathy dominates membrane protein response to detergent solubilization. Biochemistry, 51(31), 6228-6237.
146. Almeida, F. C., & Opella, S. J. (1997). fd coat protein structure in membrane environments: structural dynamics of the loop between the hydrophobic trans-membrane helix and the amphipathic in-plane helix. J Mol Biol, 270(3), 481-495.
147. Buck-Koehntop, B. A., Mascioni, A., Buffy, J. J., & Veglia, G. (2005). Structure, dynamics, and membrane topology of stannin: A mediator of neuronal cell apoptosis induced by trimethyltin chloride. J Mol Biol, 354(3), 652-665.
148. Howell, S. C., Mesleh, M. F., & Opella, S. (2005). J. NMR structure determination of a membrane protein with two transmembrane helices in micelles: MerF of the bacterial mercury detoxification system. Biochemistry, 44(13), 5196-5206.
149. Call, M. E., Schnell, J. R., Xu, C., Lutz, R. A., Chou, J. J., & Wucherpfennig, K. W. (2006). The structure

of the zetazeta transmembrane dimer reveals features essential for its assembly with the T cell receptor. Cell, 127(2), 355-368.
150. Chill, J. H., Louis, J. M., Miller, C., & Bax, A. (2006). NMR study of the tetrameric KcsA potassium channel in detergent micelles. Protein Sci, 15(4), 684-698.
151. Call, M. E., Wucherpfennig, K. W., & Chou, J. J. (2010). The structural basis for intramembrane assembly of an activating immunoreceptor complex. Nat Immunol, 11(11), 1023-1029.
152. Miyamoto, K., & Togiya, K. (2011). Solution structure of LC4 transmembrane segment of CCR5. PLoS One, 6(5), e20452.
153. Franzin, C. M., Teriete, P., & Marassi, F. M. (2007). Structural similarity of a membrane protein in micelles and membranes. J Am Chem Soc, 129(26), 8078-8079.
154. Teriete, P., Franzin, C. M., Choi, J., & Marassi, F. M. (2007). Structure of the Na,K ATPase regulatory protein FXYD1 in micelles. Biochemistry, 46(23), 6774-6783.
155. Gong, X. M., Ding, Y., Yu, J., Yao, Y., & Marassi, F. M. (2015). Structure of the Na,K-ATPase regulatory protein FXYD2b in micelles: implications for membrane-water interfacial arginines. Biochim Biophys Acta, 1848(1 Pt B), 299-306.
156. Takei, K., Tsuto, K., Miyamoto, S., & Wakatsuki, J. (1985). Anionic surfactants: Lauric products. J Am Oil Chem Soc, 62, 341-347.
157. Mitsuda, Y., & Kono, J. (2012). Anionic surfactant compositions with good fluidity and storage stability. Japan patent, 2012092163.
158. Mészaros, R., Varga, I., & Gilanyi, T. (2005). Effect of polymer molecular weight on the polymer/surfactant interaction. J Phys Chem B, 109(28), 13538-13544.
159. Yamamoto, G. (2000). Preparation of sulfuric acid esters for anionic surfactants. Japan patent, 2000247947.
160. van Heyningen, W. E., Rittenberg, D., & Schoenheimer, R. (1938). The preparation of fatty acids containing deuterium. J Biol Chem, 125, 495-500.
161. Hsiao, C. Y., Ottaway, C. A., & Wetlaufer, D. B. (1974). Preparation of fully deuterated fatty acids by simple method. Lipids, 9(11), 913-915.
162. Persky, A., & Kuppermann, A. (1974). An apparatus for the production of high isotopic purity deuterium, J Phys E: Scientific Instruments, 7, 889-890.
163. Török, Z., Szalontai, B., Joó, F., Wistrom, C. A., & Vigh, L. (1993). Homogeneous catalytic deuteration of fatty acyl chains as a tool to detect lipid phase transitions in specific membrane domains: A Fourier Transform Infrared spectroscopic study. Biochem Biophys Res Commun, 192(2), 518-524.
164. Atzrodt, J., Derdau, V., Fey, T., & Zimmermann, J. (2007). The renaissance of H/D exchange. Angew Chem Int Ed, 46(41), 7744-7765.
165. Arseniev, A. S., Barsukov, I. L., Bystrov, V. F., Lomize, A. L., & Ovchinnikov, YuA. (1985). ^{1}H-NMR study of gramicidin A transmembrane ion channel. Head-to-head right-handed, single-stranded helices. FEBS Lett. 1985;186(2):168-74.
166. Bystrov, V. F., Arseniev, A. S., Barsukov, I. L., & Lomize, A. L. (1986). 2D NMR of single and double stranded helices of gramicidin A in micelles and solutions. Bull Magn Reson, 8(3-4), 84-94.
167. Tang, P., Simplaceanu, V., & Xu, Y. (1999). Structural consequences of anesthetic and nonimmobilizer interaction with gramicidin A channels. Biophys J, 76(5), 2346-2350.
168. O'Neil, J. D., & Sykes, B. D. (1989). Side-chain dynamics of a detergent-solubilized membrane protein: measurement of tryptophan and glutamine hydrogen-exchange rates in M13 coat protein by ^{1}H NMR spectroscopy. Biochemistry, 28(16), 6736-6745.
169. Zhou, F. X., Cocco, M. J., Russ, W. P., Brunger, A. T., & Engelman, D. M. (2000). Interhelical hydrogen bonding drives strong interactions in membrane proteins. Nat Struct Biol, 7(2), 154-160
170. Hori, Y., Demura, M., Iwadate, M., Ulrich, A. S., Niidome, T., Aoyagi, H., & Asakura, T. (2001). Interaction of mastoparan with membranes studied by ^{1}H-NMR spectroscopy in detergent micelles and by solid-state ^{2}H-NMR and ^{15}N-NMR spectroscopy in oriented lipid bilayers. Eur J Biochem, 268(2), 302-309.
171. Miskolzie, M., Lucyk, S., & Kotovych, G. (2003). NMR conformational studies of micelle-bound orexin-B: a neuropeptide involved in the sleep/awake cycle and feeding regulation. J Biomol Struct Dyn, 21(3), 341-351.
172. Demura, M., Yoshida, T., Hirokawa, T., Kumaki, Y., Aizawa, T., Nitta, K., Bitter, I., & Tóth, K. (2005). Interaction of dopamine and acetylcholine with an amphiphilic resorcinarene receptor in aqueous micelle system. Bioorg Med Chem Lett, 15(5), 1367-1370.
173. Liu, L., Westler, W. M., den Boon, J. A., Wang, X., Diaz, A., Steinberg, H. A., & Ahlquist, P. (2009). An amphipathic alpha-helix controls multiple roles of brome mosaic virus protein 1a in RNA replication complex assembly and function. PLoS Pathog, 5(3), e1000351.
174. Huang, C., Mohanty, S., & Banerjee, M. (2010). A novel method of production and biophysical characterization of the catalytic domain of yeast oligosaccharyl transferase. Biochemistry, 49(6), 1115-1126.
175. Gayen, S., Li, Q., Kim, Y. M., & Kang, C. (2013). Structure of the C-terminal region of the Frizzled receptor 1 in detergent micelles. Molecules, 18(7), 8579-8590.
176. Bay, D. C., Budiman, R. A., Nieh, M. P., & Turner, R. J. (2010). Multimeric forms of the small multidrug resistance protein EmrE in anionic

detergent. Biochim Biophys Acta, 1798(3), 526-535.
177. Roosild, T. P., Greenwald, J., Vega, M., Castronovo, S., Riek, R., & Choe, S. (2005). NMR structure of Mistic, a membrane-integrating protein for membrane protein expression. Science, 307(5713), 1317-1321.
178. Bayrhuber, M., Meins, T., Habeck, M., Becker, S., Giller, K., Villinger, S., Vonrhein, C., Griesinger, C., Zweckstetter, M., & Zeth, K. (2008). Structure of the human voltage-dependent anion channel. Proc Natl Acad Sci USA, 105(40), 15370-15375.
179. Hiller, S., Garces, R. G., Malia, T. J., Orekhov, V. Y., Colombini, M., & Wagner, G. (2008). Solution structure of the integral human membrane protein VDAC-1 in detergent micelles. Science, 321(5893), 1206-1210.
180. Bondarenko, V., Mowrey, D., Tillman, T., Cui, T., Liu, L. T., Xu, Y., & Tang, P. (2012). NMR structures of the transmembrane domains of the a4b2 nAChR. Biochim Biophys Acta, 1818(5), 1261-1268.
181. Orädd, G., Lindblom, G., Arvidson, G., & Gunnarsson, K. (1995). Phase equilibria and molecular packing in the N,N-dimethyldodecylamine oxide/gramicidin D/water system studied by ^{2}H nuclear magnetic resonance spectroscopy. Biophys J, 68(2), 547-557.
182. Renaud, R. N., & Leitch, L. C. (1968). Reinvestigation of the Polonovski reaction. Synthesis of deuterated dimethylamine and formaldehyde. Can J Chem, 46, 385-390.
183. Walther, R., Fahlbusch, K., Sievert, R., & Gottschalk, G. (1981). Formation of trideuteromethane from deuterated trimethylamine or methylamine by *Methanosarcina barkeri*. J Bacteriol, 148(1), 371-373.
184. Holding, A. F. C., & Ross, W. A. (1958). The laboratory preparation of lithium deuteride and lithium aluminium deuteride, J Appl Chem, 8(5), 321-324.
185. Ujwal, R., Cascio, D., Colletier, J. P., Faham, S., Zhang, J., Toro, L., Ping, P., & Abramson, J. (2008). The crystal structure of mouse VDAC1 at 2.3 A resolution reveals mechanistic insights into metabolite gating. Proc Natl Acad Sci U S A, 105(46), 17742-17747.
186. Pebay-Peyroula, E., Garavito, R. M., Rosenbusch, J. P., Zulauf, M., & Timmins, P. A. (1995). Detergent structure in tetragonal crystals of OmpF porin. Structure, 3(10), 1051-1059.
187. Cowan, S. W., Garavito, R. M., Jansonius, J. N., Jenkins, J. A., Karlsson, R., König, N., Pai, E. F., Pauptit, R. A., Rizkallah, P. J., Rosenbusch, J. P., Rummel, G., & Schirmer, T. (1995). The structure of OmpF porin in a tetragonal crystal form. Structure, 3(10), 1041-1050.
188. Moreland, J. L., Gramada, A., Buzko, O. V., Zhang, Q., & Bourne, P. E. (2005). The Molecular Biology Toolkit (MBT): A modular platform for developing molecular visualization applications. BMC Bioinformatics, 6: 21.
189. Keana, J. F., & Roman, R. B. (1978). Improved synthesis of n-octyl-beta-D-glucoside: A nonionic detergent of considerable potential in membrane biochemistry. Membr Biochem, 1(3-4), 323-327.
190. Rosevear, P., VanAken, T., Baxter, J., & Ferguson-Miller, S. (1980). Alkyl glycoside detergents: a simpler synthesis and their effects on kinetic and physical properties of cytochrome c oxidase. Biochemistry, 19(17), 4108-4115.
191. Koch, H. J., & Stuart, R. S. (1978). The synthesis of per-C-deuterated D-glucose. Carbohyd Res, 64:127-134.
192. Yoshimura, Y., Shimizu, H., Hiroshi Hinoub, H., & Nishimura, S.-I. (2005). A novel glycosylation concept; microwave-assisted acetal-exchange type glycosylations from methyl glycosides as donors. Tet Lett, 46(28), 4701-4705.
193. Hwang, P. M., Choy, W. Y., Lo, E. I., Chen, L., Forman-Kay, J. D., Raetz, C. R., Privé, G. G., Bishop, R. E., & Kay, L. E. (2002). Solution structure and dynamics of the outer membrane enzyme PagP by NMR. Proc Natl Acad Sci USA, 99(21), 13560-13565.
194. Gabel, F., Lensink, M. F., Clantin, B., Jacob-Dubuisson, F., Villeret, V., & Ebel, C. (2014). Probing the conformation of FhaC with small-angle neutron scattering and molecular modeling. Biophys J, 107(1), 185-196.
195. Clantin, B., Delattre, A. S., Rucktooa, P., Saint, N., Méli, A. C., Locht, C., Jacob-Dubuisson, F., & Villeret, V. (2007). Structure of the membrane protein FhaC: A member of the Omp85-TpsB transporter superfamily. Science, 317(5840), 957-961.
196. Midtgaard, S. R., Darwish, T. A., Pedersen, M. C., Huda, P., Larsen, A. H., Jensen, G. V., Kynde, S. A. R., Skar-Gislinge, N., Nielsen, A. J. Z., Olesen, C., Blaise, M., Dorosz, J. J., Thorsen, T. S., Venskutonytė, R., Krintel, C., Møller, J. V., Frielinghaus, H., Gilbert, E. P., Martel, A., Kastrup, J. S., Jensen, P. E., Nissen, P., & Arleth, L. (2018). Invisible detergents for structure determination of membrane proteins by small-angle neutron scattering. FEBS J, 285(2), 357-371.
197. Cleveland Iv, T., Blick, E., Krueger, S., Leung, A., Darwish, T., & Butler, P. (2021). Direct localization of detergents and bacteriorhodopsin in the lipidic cubic phase by small-angle neutron scattering. IUCrJ, 8(Pt 1), 22-32.
198. Ward, A., Sanderson, N. M., O'Reilly, J., Rutherford, N. G., Poolman, B., & Henderson, P. J. F. (2000). The amplified expression, identification, purification, assay and properties of hexahistidine tagged bacterial membrane transport proteins. In: Baldwin SA (Ed). Membrane transport– a practical approach. Oxford: Blackwell, 141-166.
199. Pagliano, C., Barera, S., Chimirri, F., Saracco, G., & Barber, J. (2012). Comparison of the α and β

isomeric forms of the detergent n-dodecyl-D-maltoside for solubilizing photosynthetic complexes from pea thylakoid membranes. Biochim Biophys Acta, 1817(8), 1506-1515.
200. Rouse, S. L., Marcoux, J., Robinson, C. V., & Sansom, M. S. (2013). Dodecyl maltoside protects membrane proteins in vacuo. Biophys J, 105(3), 648-656.
201. Ma, P., Patching, S. G., Ivanova, E., Baldwin, J. M., Sharples, D., Baldwin, S. A., & Henderson, P. J. (2016). Allantoin transport protein, PucI, from *Bacillus subtilis*: Evolutionary relationships, amplified expression, activity and specificity. Microbiology, 162(5), 823-836.
202. Rahman, M., Ismat, F., Jiao, L., Baldwin, J. M., Sharples, D. J., Baldwin, S. A., & Patching, S. G. (2017). Characterisation of the DAACS family Escherichia coli glutamate/aspartate-proton symporter GltP using computational, chemical, biochemical and biophysical methods. J Membr Biol, 250(2), 145-162.
203. Newstead, S., Ferrandon, S., & Iwata, S. (2008). Rationalizing alpha-helical membrane protein crystallization. Protein Sci, 17(3), 466-472.
204. Parker, J. L., & Newstead, S. (2012). Current trends in α-helical membrane protein crystallization: An update. Protein Sci, 21(9), 1358-1365.
205. He, Y., Wang, K., & Yan, N. (2014). The recombinant expression systems for structure determination of eukaryotic membrane proteins. Protein Cell, 5(9), 658-672.
206. Takeuchi, K., Takahashi, H., Kawano, S., & Shimada, I. (2007). Identification and characterization of the slowly exchanging pH-dependent conformational rearrangement in KcsA. J Biol Chem, 282(20), 15179-15186.
207. Calcutta, A., Jessen, C. M., Behrens, M. A., Oliveira, C. L., Renart, M. L., González-Ros, J. M., Otzen, D. E., Pedersen, J. S., Malmendal, A., & Nielsen, N. C. (2012). Mapping of unfolding states of integral helical membrane proteins by GPS-NMR and scattering techniques: TFE-induced unfolding of KcsA in DDM surfactant. Biochim Biophys Acta, 1818(9), 2290-2301.
208. Chung, K. Y., Kim, T. H., Manglik, A., Alvares, R., Kobilka, B. K., & Prosser, R. S. (2012). Role of detergents in conformational exchange of a G protein-coupled receptor. J Biol Chem, 287(43), 36305-36311.
209. Li, G. C., Castro, M. A., Ukwaththage, T., & Sanders, C. R. (2024). Optimizing NMR fragment-based drug screening for membrane protein targets. J Struct Biol X, 9, 100100.
210. Mendoza-Hoffmann, F., Guo, C., Song, Y., Feng, D., Yang, L., & Wüthrich, K. (2024). ^{19}F-NMR studies of the impact of different detergents and nanodiscs on the A2A adenosine receptor. J Biomol NMR, 78(1), 31-37.
211. Hines, H. D., Thomas, R. K., Garrett, P. R., Rennie, G. K., & Penfold, J. (1997). Investigation of mixing in binary surfactant solutions by surface tension and neutron reflection: Anionic/nonionic and zwitterionic/nonionic mixtures. J Phys Chem B, 101(45), 9215-9223.
212. Vacklin, H. P., Tiberg, F., T& homas, R. K. (2005). Formation of supported phospholipid bilayers via co-adsorption with beta-D-dodecyl maltoside. Biochim Biophys Acta – Biomembr, 1668(1), 17-24.
213. Patzelt, H., Simon, B., terLaak, A., Kessler, B., Kühne, R., Schmieder, P., Oesterhelt, D., & Oschkinat, H. (2002). The structures of the active center in dark-adapted bacteriorhodopsin by solution-state NMR spectroscopy. Proc Natl Acad Sci U S A, 99(15), 9765-9770.
214. Schubert, M., Kolbe, M., Kessler, B., Oesterhelt, D., & Schmieder, P. (2002). Heteronuclear multidimensional NMR spectroscopy of solubilized membrane proteins: Resonance assignment of native bacteriorhodopsin. Chembiochem, 3(10), 1019-1023.
215. Imai, S., Osawa, M., Takeuchi, K., & Shimada, I. (2010). Structural basis underlying the dual gate properties of KcsA. Proc Natl Acad Sci USA, 107(14), 6216-6221.
216. Vacklin, H. P., Tiberg, F., Fragneto, G., & Thomas, R. K. (2005). Composition of supported model determined by neutron reflection. Langmuir, 21(7):2827-2837.
217. Ciaccafava, A., De Poulpiquet, A., Infossi, P., Robert, S., Gadiou, R., Giudici Orticoni, M. T., Lecomte, S., & Lojou, E. (2012). A friendly detergent for H2 oxidation by *Aquifex aeolicus* membrane-bound hydrogenase immobilized on graphite and Self-Assembled-Monolayer-modified gold electrode. Electrochimica Acta, 82, 115-125.
218. Hiruma-Shimizu, K., Kalverda, A. P., Henderson, P. J. F., Homans, S. W., & Patching, S. G. (2014). Synthesis of uniformly deuterated n-dodecyl-β-D-maltoside (d_{39}-DDM) for solubilisation of membrane proteins in TROSY NMR experiments. J Label Compd Radiopharm, 57(14), 737-743.
219. Lycksell, M., Rovšnik, U., Bergh, C., Johansen, N. T., Martel, A., Porcar, L., Arleth, L., Howard, R. J., & Lindahl, E. (2021). Probing solution structure of the pentameric ligand-gated ion channel GLIC by small-angle neutron scattering. Proc Natl Acad Sci U S A, 118(37), e2108006118.
220. Golub, M., Gätcke, J., Subramanian, S., Kölsch, A., Darwish, T., Howard, J. K., Feoktystov, A., Matsarskaia, O., Martel, A., Porcar, L., Zouni, A., & Pieper, J. (2022). "Invisible" detergents enable a reliable determination of solution structures of native photosystems by small-angle neutron scattering. J Phys Chem B, 126(15), 2824-2833.
221. Oliver, R. C., Pingali, S. V., & Urban, V. S. (2017). Designing mixed detergent micelles for uniform neutron contrast. J Phys Chem Lett, 8(20), 5041-5046.

222. Naing, S. H., Oliver, R. C., Weiss, K. L., Urban, V. S., & Lieberman, R. L. (2018). Solution structure of an intramembrane aspartyl protease via small angle neutron scattering. Biophys J, 114(3), 602-608.
223. Martin, R., Larsen, A. H., Corey, R. A., Midtgaard, S. R., Frielinghaus, H., Schaffitzel, C., Arleth, L., & Collinson, I. (2019). Structure and dynamics of the central lipid pool and proteins of the bacterial holo-translocon. Biophys J, 116(10), 1931-1940.
224. Arora, A., Abildgaard, F., Bushweller, J. H., & Tamm, L. K. (2001). Structure of outer membrane protein A transmembrane domain by NMR spectroscopy. Nat Struct Biol, 8(4), 334-338.
225. Cierpicki, T., Liang, B., Tamm, L. K., & Bushweller, J. H. (2006). Increasing the accuracy of solution NMR structures of membrane proteins by application of residual dipolar couplings. High-resolution structure of outer membrane protein A. J Am Chem Soc, 128(21), 6947-6951.
226. Liang, B., & Tamm, L. K. (2007). Structure of outer membrane protein G by solution NMR spectroscopy. Proc Natl Acad Sci USA, 104(41), 16140-16145.
227. Hagn, F., Etzkorn, M., Raschle, T., & Wagner, G. (2013). Optimized phospholipid bilayer nanodiscs facilitate high-resolution structure determination of membrane proteins. J Am Chem Soc, 135(5), 1919-1925.
228. Fox, D. A., Larsson, P., Lo, R. H., Kroncke, B. M., Kasson, P. M., & Columbus, L. (2014). Structure of the neisserial outer membrane protein Opa60: Loop flexibility essential to receptor recognition and bacterial engulfment. J Am Chem Soc, 136, 9938-9946.
229. Oxenoid, K., & Chou, J. J. (2005). The structure of phospholamban pentamer reveals a channel-like architecture in membranes. Proc Natl Acad Sci USA, 102(31), 10870-10875.
230. Yu, L., Sun, C., Song, D., Shen, J., Xu, N., Gunasekera, A., Hajduk, P. J., & Olejniczak, E. T. (2005). Nuclear magnetic resonance structural studies of a potassium channel-charybdotoxin complex. Biochemistry, 44(48), 15834-15841.
231. Zhou, Y., Cierpicki, T., Jimenez, R. H., Lukasik, S. M., Ellena, J. F., Cafiso, D. S., Kadokura, H., Beckwith, J., & Bushweller, J. H. (2008). NMR solution structure of the integral membrane enzyme DsbB: Functional insights into DsbB-catalyzed disulfide bond formation. Mol Cell, 31(6), 896-908.
232. van Horn, W. D., Kim, H. J., Ellis, C. D., Hadziselimovic, A., Sulistijo, E. S., Karra, M.D., Tian, C., Sönnichsen, F. D., & Sanders, C. R. (2009). Solution nuclear magnetic resonance structure of membrane-integral diacylglycerol kinase. Science, 324(5935), 1726-1729.
233. Shenkarev, Z. O., Paramonov, A. S., Lyukmanova, E. N., Shingarova, L. N., Yakimov, S. A., Dubinnyi, M. A., Chupin, V. V., Kirpichnikov, M. P., Blommers, M. J., & Arseniev AS. (2010). NMR structural and dynamical investigation of the isolated voltage-sensing domain of the potassium channel KvAP: Implications for voltage gating. J Am Chem Soc, 132(16), 5630-5637.
234. Montserret, R., Saint, N., Vanbelle, C., Salvay, A. G., Simorre, J. P., Ebel, C., Sapay, N., Renisio, J. G., Böckmann, A, Steinmann, E., Pietschmann, T., Dubuisson, J., Chipot, C., & Penin, F. (2010). NMR structure and ion channel activity of the p7 protein from hepatitis C virus. J Biol Chem, 285(41), 31446-31461.
235. OuYang, B., Xie, S., Berardi, M. J., Zhao, X., Dev, J., Yu, W., Sun, B., & Chou, J. J. (2013). Unusual architecture of the p7 channel from hepatitis C virus. Nature, 498(7455), 521-525.
236. Berardi, M. J., Shih, W. M., Harrison, S. C., & Chou, J. J. (2011). Mitochondrial uncoupling protein 2 structure determined by NMR molecular fragment searching. Nature, 476(7358), 109-113.
237. Magolda, R. L., & Johnson, P. R. (1985). A new efficient and versatile synthesis of alkyl phosphorylcholines. Tet Lett, 26, 1167-1170.
238. Leitch, L. C., & Morse, A. T. (1952). Synthesis of organic deuterium compounds III. 1,2-dibromoethane-d and its derivatives. Can J Chem, 30(12), 924-932.
239. Pautsch, A., & Schulz, G. E. (1998). Structure of the outer membrane protein A transmembrane domain. Nat Struct Biol, 5(11), 1013-1017.
240. Pautsch, A., & Schulz, G. E. (2000). High-resolution structure of the OmpA membrane domain. J Mol Biol, 298(2), 273-282.
241. Nadezhdin, K. D., Bocharova, O. V., Bocharov, E. V., & Arseniev, A. S. (2011). Structural and dynamic study of the transmembrane domain of the amyloid precursor protein. Acta Naturae, 3(1), 69-76.
242. Chen, W., Gamache, E., Rosenman, D. J., Xie, J., Lopez, M. M., Li, Y. M., & Wang, C. (2014). Familial Alzheimer's mutations within APPTM increase Ab42 production by enhancing accessibility of e-cleavage site. Nat Commun, 5, 3037.
243. Vostrikov, V. V., Mote, K. R., Verardi, R., & Veglia, G. (2013). Structural dynamics and topology of phosphorylated phospholamban homopentamer reveal its role in the regulation of calcium transport. Structure, 21(12), 2119-2130.
244. Roche, J., Louis, J. M., Grishaev, A., Ying, J., & Bax, A. (2014). Dissociation of the trimeric gp41 ectodomain at the lipid-water interface suggests an active role in HIV-1 Env-mediated membrane fusion. Proc Natl Acad Sci USA, 111(9), 3425-3430.
245. Reardon, P. N., Sage, H., Dennison, S. M., Martin, J. W., Donald, B. R., Alam, S. M., Haynes, B. F., & Spicer, L. D. (2014). Structure of an HIV-1-neutralizing antibody target, the lipid-bound gp41 envelope membrane proximal region trimer. Proc Natl Acad Sci USA, 111(4), 1391-1396.
246. Jaremko, L., Jaremko, M., Giller, K., Becker, S., & Zweckstetter, M. (2014). Structure of the

mitochondrial translocator protein in complex with a diagnostic ligand. Science, 343(6177), 1363-1366.
247. Zhou, S., Pettersson, P., Huang, J., Sjöholm, J., Sjöstrand, D., Pomès, R., Högbom, M., Brzezinski, P., Mäler, L., & Ädelroth, P. (2018). Solution NMR structure of yeast Rcf1, a protein involved in respiratory supercomplex formation. Proc Natl Acad Sci U S A, 115, 3048-3053.
248. Vincent, M. S., Comas Hervada, C., Sebban-Kreuzer, C., Le Guenno, H., Chabalier, M., Kosta, A., Guerlesquin, F., Mignot, T., McBride, M. J., Cascales, E., & Doan, T. (2022). Dynamic proton-dependent motors power type IX secretion and gliding motility in Flavobacterium. PLoS Biol, 20(3), e3001443.
249. Tulumello, D. V., & Deber, C. M. (2012). Efficiency of detergents at maintaining membrane protein structures in their biologically relevant forms. Biochim Biophys, 1818(5), 1351-1358.
250. Patching, S. G. (2025). Ultra-high field nuclear magnetic resonance (NMR) spectroscopy: Applications at 1 GHz and beyond. Int J Curr Sci Res Rev, 8(1), 336-351.